NASA TECHNICAL MEMORANDUM 102755
AVSCOM TECHNICAL MEMORANDUM 90-B-018

RESPONSE OF COMPOSITE MATERIALS TO LOW VELOCITY IMPACT

K. Srinivasan, W.C. Jackson and J. A. Hinkley

JANUARY 1991

NASA

National Aeronautics and
Space Administration

Langley Research Center
Hampton, Virginia 23665

US ARMY
AVIATION
SYSTEMS COMMAND
AVIATION R&T ACTIVITY

RESPONSE OF COMPOSITE MATERIALS TO LOW VELOCITY IMPACT

K. SRINIVASAN[1], W. C. JACKSON[2] AND J. A. HINKLEY[3]

I. INTRODUCTION

Composite materials made of continuous carbon fibers and high performance polymers are gaining increasing acceptance in aerospace structures due to potential weight savings and efficient design considerations. However foreign object impact damage has been identified as a serious constraint limiting widespread use of these materials. As the first generation of epoxy based composites was extremely susceptible to impact damage (with attendant mechanical property losses), newer damage tolerant and damage resistant resins have been formulated for composite applications. It is not always clear, however, what properties of the neat resin (or composite) lead to the improvements in impact behavior. Further, the two widely-followed tests of impact damage tolerance require very large amounts of material for testing. Finally, impact data is lacking on the newer resins coupled with recently introduced high strain, intermediate modulus carbon fibers. This study seeks to address these three issues.

Impact damage tolerance of composites has received much attention [1-10]. These studies have shown that many properties may be considerably degraded by low velocity impacts that do not even cause visible damage. Recently, most impact tests have been instrumented

----

[1] Research Associate, Department of Mechanical Engineering and Mechanics, Old Dominion University, Norfolk, VA 23529-0247.
[2] Aerospace Engineer, US Army Aerostructures Directorate (AVSCOM), NASA Langley Research Center, Hampton, VA 23665-5225.
[3] Physical Chemist, Materials Division, NASA Langley Research Center, Hampton, VA 23665-5225.

to provide a wealth of information on the force, displacement and energy absorbing characteristics of the material while it is undergoing the impact event [11]. Several methods exist to evaluate the damage caused by the impact event. These include residual compression strength, residual tensile strength [12], post - impact fatigue behavior [13], cross-sectional microscopic observations [9], deplying [7], X-ray radiography [10], ultrasonic C-Scanning, 3-D acoustic scanning etc.

Two types of tests have emerged as leading candidates for impact damage evaluation in composite materials. The NASA standard test [14] employs a fired ball on a 48 ply composite plate target to simulate the impact event, while the Boeing test [4] uses a drop weight assembly to impact a 32 ply laminate. Both attempt to use different mass-velocity combinations to achieve the same incident impact energy on quasi-isotropic plates with widely differing results. The NASA test is a more conservative predictor of compression after impact (CAI) behavior. However, the drop weight test readily lends itself to instrumentation that captures the impact force - displacement - energy profiles during the impact event.

The goal of the present study is to evaluate the impact damage resistance and residual compressive strength of various composite systems and to compare the effect of material characteristics on impact damage tolerance. This would help elucidate key neat resin/composite properties that are responsible for specific enhancement of impact damage tolerance. Both the NASA and Boeing tests require large amounts of material for testing, which is not a feasible option for evaluating potential new resin systems. Hence an auxiliary objective of this study is to find a small scale test that mimics the CAI behavior of composites.

II. TECHNICAL APPROACH

Since the objective of this study was to determine neat resin characteristics that affected the impact resistance of composites, systems representing generic classes of polymeric behavior were selected for this study. These comprised a brittle epoxy (baseline material),

toughened epoxies (both co-continous and discrete-phase types) and thermoplastics (both amorphous and semi-crystalline). These materials possessed widely different chemistries, processing operations, deformational capabilities and morphological and microstructural profiles. Thus it was anticipated that from this study, a better picture of toughening in composites could be formulated. One material, reinforced with different grades of carbon fiber, was also studied to determine the influence of the newer, high strain fiber on the impact properties of composites.

Many investigators studying impact have utilized simply supported specimen plate conditions [15], while still others [16-18], have employed fully clamped or membrane clamping between edge supports as end conditions. The latter two are more representative of real structures. Husman *et al.* [19] have shown, that in general, specimen width to projectile diameter ratio must be at least six or greater to simulate infinite plate conditions. These factors were helpful in determining both the geometry and size of specimens utilized in the study.

Though the fired projectile test is a more realistic predictor of impact resistance, particularly in flight operations, it cannot be easily configured to provide force - displacement - energy profiles during the impact event. Hence, due to the ease of instrumentation, the drop weight geometry was employed, in order to obtain the deformational response of the materials during the impact event. This was deemed particularly important as this study focussed on understanding impact resistance/tolerance in composite materials.

In order to provide ready comparisons between the data obtained in this study and impact data (both Boeing and NASA results) available in the literature, most of the data was generated on quasi-isotropic laminates. Further, to minimize material used in the test, 24-ply laminates were utilized for the bulk of the characterization. A limited number of tests were also conducted on 48-ply laminates, primarily for comparisons with the results on 24-ply samples. Finally, limited tests were also conducted on 24-ply orthotropic laminates.

III. MATERIALS AND TEST PROCEDURES

1. Materials

The materials selected for evaluation were:

MATERIAL	SUPPLIER	LAMINATE FIBER VOLUME %
3501-6/AS-4	Hercules	59.5
977-2/IM-7	ICI	61.0
T3900-2/T800-H	Hexcel	58.4
PEEK/AS-4	ICI	63.0
PEEK/IM-7	ICI	62.9
ULTEM1000/AS-4	In-House	56.8

The first material was used as a baseline material, since it is in wide commercial use and represents a highly crosslinked brittle epoxy. The 977-2 and T3900-2 materials represent various approaches to toughening thermosets; one being a co-continous network (977-2), while the other is a particulate-toughened system. The last three materials represent thermoplastic polymer matrix composites; PEEK being semicrystalline and Ultem representing an amorphous polyimide. The PEEK material was available with two types of reinforcing fibers : AS-4 and the newer IM-7.

All materials were processed in house according to manufacturer specifications. Laminates were 24 and 48 ply quasi-isotropic plates with a layup designation of $(-45/0/45/90)_{ns}$. Specimens, 4.75 in. X 4.0 in. were then cut from these plates, with the 0 degree direction along the longer specimen direction. Some 24 ply $(0/90)_{6s}$ laminates were also made with the PEEK material in order to effect a comparison between the orthotropic and quasi-isotropic laminates. Typical thicknesses ranged from 0.123 in. to 0.146 in. for the 24 ply and from 0.255 to 0.284 in. for the 48 ply samples. All sample edges were ground to ensure flat and perpendicular faces. Routine C-scans were performed to ensure that samples were free of gross defects prior to the impact test.

2. Experimental Procedures

The fixture (figure 1) consisted of a pair of 6 in. square picture frame blocks, made of mild steel, each 0.75 in. thick and having a central 3 in. X 3 in. cutout. The sample was clamped between the two blocks by ten 1/4-20 engineering bolts, each torqued to 100 in.-lb. Verpoest et al. [20] have suggested that the influence of clamping force is negligible on the outcome of the impact test. The sample was aligned so as to be impacted at the center of the plate.

The instrumented drop weight tester (figure 2) consisted of a 6.05 lb. striker with a 0.5 in.-diameter stainless steel tup. Attached to the striker was a 50 line/inch grating flag. As the striker descended through the guide tube, the flag intercepted a collimated beam of laser light just prior to the impact. The resulting signal from a PIN LSC-30D photoelectric detector allowed precise measurement of the impact and rebound velocities. The striker was instrumented to measure both load (via a strain gage assembly) and acceleration. Data was recorded on a high speed four channel Nicolet Digital storage oscilloscope. The incident impact energy on the specimen was changed by varying the drop height of the striker in the guide tube. At least six different heights were employed for each material. After impact, the specimens were C-scanned to determine damage profiles. Some samples were photographed to preserve a record of the visual damage. Certain samples were sectioned, polished and viewed through an optical microscope to view the damage patterns due to the impact. A large majority of the samples were then instrumented with six back-to-back strain gages each (four Longitudinal and two Poisson) as shown in figure 3. These were then subject to plate compression in an edge supported compression fixture, at a crosshead rate of 0.04 in. per min. This procedure was used to establish CAI strengths and strains.

A specific computer program was used to analyze the raw impact data. Briefly, the load data was integrated to get the velocity, which was then integrated to get the displacement. Several other parameters such as energy profiles during the impact, load-drops, slope changes and peak loads and displacements were also calculated. A typical smoothed load-displacement curve generated during an impact test is shown in figure 4; the terminology employed is explained subsequently in detail.

IV. RESULTS AND DISCUSSION

1.   24-Ply Quasi-Isotropic Laminate Results

Figure 5 depicts a planar measure of the extent of delamination (determined by C-Scan tests) in the composite samples as a function of the incident impact energy on the plate. Though it discounts delaminated areas that lie on top of one another, it is still instructive from a materials classification viewpoint. Several features are worth noting from the graph. Firstly, for identical energies of impact, the epoxy material shows the greatest damage while the Ultem polyimide material shows the least. This is important when considering the relative damage resistances of the different materials. Secondly, the slope of the plot for each material (except T3900-2 and Ultem) increases continuously with impact energy (*i.e.*, the rate of damage creation increases with the incident impact energy). Further, the divergence in the C-Scan areas among these materials is most significant at the higher impact energies. The difference between the PEEK/IM-7 and PEEK/AS-4 materials appears negligible, implying that the damage resistance to impact is a strong function of the matrix material.

A typical load-displacement curve for a sample undergoing impact is shown in figure 4. If, as in this case, the incident impact energy is sufficiently high, then a load drop is seen. This sudden drop is accompanied by an audible crack. The load and displacement values at the onset of the load drop are termed the breaking load and displacement respectively. The load values at the peak and trough of the load drop are used to compute the extent of the load drop. The peak load and displacement seen by the sample during the impact are also marked. Finally, a bending stiffness change is computed by subtracting the slopes of the loading and unloading curves, determined as shown in the figure at a displacement of 0.01 in. from the load-free displacements.

Figures 6 and 7 are plots of the breaking loads and displacements as a function of the impact energy. Though each material shows a different level of load and displacement at which the load drop occurs, for any material, both remain constant as the impact energy is increased. Optical

6

microscopy indicates that samples that have undergone a load drop display extensive delaminations. This implies that below a certain characteristic material-dependent load/displacement value, no impact-induced delaminations appear, but above it, delamination damage is seen. This observation indicates that one of the intermediate steps in the impact damage pattern is the formation of a characteristic damage state, that subsequently grows as the load/displacement rises beyond the breaking load/displacement value (as indicated by figure 5).

Figure 8 presents the changes in dynamic bending stiffness observed for the different systems. From this figure it is evident that in all materials, impacts can lead to severe stiffness losses. At low impact energies, below those that cause damage, the bending stiffness is virtually unchanged. However beyond a certain (material dependent) threshold energy, there is a dramatic increase in stiffness loss. At higher energies the rate of increase of the stiffness change tapers off sharply. Thus, though the damage area continues to increase with increasing impact energy, (Figure 5), the bending stiffness loss depends mostly on a characteristic damage state created during the impact event. The subsequent growth of the damage during the test has very little incremental influence on the bending stiffness loss. Greater incident impact energies than that corresponding to the threshold level cause very little additional stiffness loss. That the threshold values are different in these materials, suggests that this could be a valuable measure of impact damage resistance in these materials.

Figure 9 depicts the extent of the load drops observed at the first failure event as a function of the incident impact energy. Two distinct patterns of behavior are observed. The 3501-6 and 977-2 materials show a constant load drop as a function of the incident impact energy. Since the load drop is related to the area of damage created, this constant load drop implies that irrespective of the incident impact energy, a characteristic damage area is created. As the load increases during the test, this damage area continues to grow. However, the PEEK, 3900-2 and Ultem 1000 materials show increasing load drops as the impact energy is increased, implying that the area of damage creation is dependent on the incident impact energy. Since the drop occurs at a constant value of load/displacement in each of these materials, this behavior indicates the rate dependent behavior of these materials during the impact event. At increasing impact energies (*i.e.*

increasing rates of loading), the characteristic damage zone is probably increasing. This subtle rate dependence has not been reported in the literature. While it is not surprising to see this rate dependency in the thermoplastics (PEEK and Ultem), its appearance in the T3900-2 material (a cross-linked system), is worthy of note.

Figures 10 and 11 show the results of plate compression tests on impact damaged specimens. For a comparison, results from the compression tests on undamaged laminates are also shown in the figures. All materials show dropoffs in compressive strength/failure strains with increasing impact energy. While the 3501-6 material shows the greatest loss of compression after impact strengths and strains, classification among the other materials is difficult particularly at the higher impact energies. The influence of the fiber on the compressive behavior is clearly evident by comparing the results of the PEEK/IM-7 and PEEK/AS-4 composites. PEEK/IM-7 laminates show greater CAI strengths and lower strains throughout the entire energy spectrum. Thus while impact damage resistance is hardly affected by fiber characteristics, the impact damage tolerance (in compression) is dependent on it. However, the matrix still exerts a dominant effect on the impact damage tolerance: witness the divergent post-impact-compression behavior of the Ultem 1000/AS-4, PEEK/AS-4 and 3501-6/AS-4 damaged laminates.

In order to gain insights into the nature of the damage suffered by the materials during impact, as well as to effect a comparison between the different materials, the results of Figs. 10 and 11 are replotted, for each of the different materials, by normalizing the compressive strengths/strains at each energy level by that of the unimpacted laminate compression strength/strain value. These results appear in figures 12 and 13. From these figures, a ranking of materials in order of the CAI strengths/strains falls into three categories. One group, consisting of the PEEK, T3900-2 and 977-2 materials, shows strength/strain losses substantially less than those of the epoxy across the entire range of impact energies studied. The Ultem polyimide material forms a third category and shows the least property degradation due to impact. An important observation from both these graphs is the fact that most of the loss in the CAI strength and strain occurs at the lower end of the impact energy spectrum. This reinforces the conclusion of the earlier results

presented, that most of the impact induced property loss is associated with the formation of a characteristic incipient damage pattern. The growth of the delaminations/matrix cracks beyond the preliminary damage state appears to have a small incremental effect in further degrading the properties of the laminate.

A review of the experimental results of the impact study on 24-ply quasi-isotropic laminates indicates that although the fiber determines the base level of composite compressive strength and the elasticity of the plate as seen in the contact duration profiles (figure 14), the matrix exerts a dominant influence on the impact response of the laminates.

2. 48-Ply Quasi-Isotropic Laminate Results

As mentioned previously, one of the main objectives of this study was to devise a CAI test that would be less material intensive than the NASA and Boeing tests. Accordingly, impact and CAI tests were run on 48-ply quasi-isotropic specimens of selected materials. All procedures followed were identical to those for the 24-ply laminates. Figures 15 to 21 depict the observed results. Although slight quantitative differences exist, the trends in properties as a function of impact energy are similar to those shown by the 24-ply laminates, and they are are interpreted similarly.

A more instructive exercise is a comparison of thickness effects on the CAI behavior of impacted laminates. This is achieved by normalizing the incident impact energy by the thickness of the plate sample. Figures 22 to 29 present the influence of plate thickness on the CAI strengths and ultimate strains for each of the four materials. When examined in this manner, the 24- and 48-ply laminate CAI strengths and strains are very similar for all four of the materials studied. Note also that the materials selected encompass a wide spectrum of composite matrix behavior, hence this seems to be a generic composite response. Damage patterns (to be discussed in a subsequent paper) were also observed to be similar. Thus in order to reduce material requirements for the CAI test, preliminary screening tests can be undertaken with 24-ply laminates.

3. 24-Ply Orthotropic Laminate Results

Availability of PEEK material permitted a limited number of tests on 24-ply $(0/90)_{6s}$ plates. Plate thicknesses were similar to those of the 24-ply quasi-isotropic specimens. All fabrication, specimen preparation and testing details were also identical. Figure 30 depicts the C-Scan damage area profiles of the orthotropic and quasi-isotropic specimens. For identical impact energies, the orthotropic plates may suffer slightly greater damage than the quasi-isotropic specimens. However the C-Scan damage areas are not significantly different, implying that the differences in the internal stress state induced by the stacking sequence play only a small role in determining the damage accrued during impact. Owing to the paucity of specimens, internal damage patterns were not examined in the orthotropic plates.

Actual CAI strengths were consistently higher in the orthotropic materials, presumably due to the higher proportion of 0° fibers. The corresponding CAI ultimate strains were lower than they were in the quasi-isotropic plates. Figures 31 and 32 compare the normalized CAI strengths and ultimate strains of the orthotropic and quasi-isotropic specimens. The normalized plots show that the scatter is greater in the orthotropic plate data. The normalized CAI strengths for the orthotropic plates are higher than those for the quasi-isotropic specimens, but the normalized CAI ultimate strains are quite similar. Both figures point to the relative insensitivity of the damage processes to the details of the internal stress state. As material requirements are considerably lower in orthotropic specimens as compared to the quasi-isotropic plates, these tests appear to be a good qualitative evaluation tool for newer materials.

4. Impact Test Comparisons

Finally, it is appropriate to provide a comparison of the results of the present test with those of the Boeing [4] and NASA [14] impact tests. Figures 33 and 34 show that the present miniaturized test is intermediate in severity between the Boeing and NASA tests. In conjunction with suitable data reduction techniques, it should therefore be a useful materials screening/evaluation tool.

V CONCLUSIONS

A review of the results of this experimental study reveals that the matrix exerts a dominant influence on the impact resistances of the composites studied. Though CAI strengths and strains are the most critical property from a design/structural viewpoint, CAI properties actually involve (from a fundamental perspective) two distinct and separate problems. The first, damage resistance, involves the flaw spectrum created in an impacted laminate; and the second, damage tolerance, concerns the compressive response of a laminate that has such a flaw spectrum. Therefore, in trying to determine the factors that influence overall behavior, it is important to distinguish between damage resistance and damage tolerance. Further, given the fact that composites always contain numerous voids and intrinsic flaws, it is important to understand the inter-relationship between damage tolerance and resistance.

From the viewpoint of damage resistance, a relative ranking (in increasing order) of the materials studied is 3501-6/AS-4 < PEEK/IM-7 < PEEK/AS-4 < 977-2/IM-7 < T3900-2/T800-H < ULTEM1000/AS-4. There is almost a factor of 8 difference between the best and the worst materials at the higher impact energies employed.

Damage tolerance is more difficult to quantify in this case; ranking by CAI strains or strengths leads to different results. Ranking by CAI strengths, one notes that all the newer materials show great improvements over the baseline epoxy behavior. However, there is virtually no difference in the CAI strength behavior at higher impact energies among the "tough" materials. Thus the large damage resistance in the T3900-2 and Ultem materials does not translate into significantly greater retention of compression properties. Another significant conclusion gleaned from comparing the PEEK/AS-4 and PEEK/IM-7 response is that the fiber is important in deciding the plate compressive properties irrespective of the impact energy levels. The IM-7 system consistently shows a 10 % increase in CAI strengths (and a corresponding dropoff in ultimate strains) over the AS-4 based material.

Since the level of CAI strength or strain can be influenced by the fiber selection, a more meaningful measure of the damage tolerance is the loss of properties as a function of incident impact energy. By this measure, both normalized CAI strengths and ultimate strains show the Ultem material to be the most damage tolerant. The 977-2, PEEK and 3900-2 materials form the next tier which is still significantly higher than that of the baseline 3501-6 epoxy composite.

From the impact load/deflection trace, one arrives at the following description of the impact event: During the test, at a material-dependent and perhaps thickness-dependent load/displacement value, damage in the form of matrix cracks and delaminations begins to appear. As the impacter continues to load the plate, this characteristic damage pattern grows. The propagation of this damage, however, has surprisingly little influence on the residual properties of the impacted laminate. Although the plot of C-Scan damage areas shows that the extent of the growth of the damage depends on the total displacement suffered during the impact event, most of the falloff in bending stiffness and in compressive properties occurs at the lower impact energies. Thus the impact behavior seems to be primarily an initiation problem, in which the losses in mechanical properties are determined by what happens during the early stages of the impact event, with the damage growth aspects being nearly irrelevant.

The load drop behavior offers useful clues into the constitutive behavior of the matrix. The increasingly brittle behavior in some of the materials at higher rates of testing is consistent with the usual behavior of polymeric materials.

Data obtained in the present study correlate reasonably well with results of standard tests while requiring significantly less prepreg. A preliminary screening test using an orthotropic layup and requiring even less material has been outlined.

ACKNOWLEDGEMENT

REFERENCES

1. Palmer, R. J. : "Investigations of the Effect of Resin Materials on the Impact Damage to Graphite/Epoxy Composites.", NASA CR 165677, March 1981.

2. Adams, D. F. : "Impact Response of Polymer Matrix Composite Materials.", Composite Materials : Testing and Design (Fourth Conference), ASTM STP 617, ASTM, 1977, pp 409 - 426.

3. Rhodes, M. D., Williams, J. G., and Starnes, J. H., : "Low Velocity Impact in Graphite Fiber Epoxy Laminates.", Proceedings of the 34th Annual Conference of Reinforced Plastics/Composites Institute, New Orleans, LA, January 30 - February 2 1979, pp 20-D1 - 20- D10.

4. SRM 2-88 "SACMA Recommended Test Method for Compression After Impact Properties of Oriented Fiber-Resin Composites" , Suppliers of Advanced Composite Materials Association

5. Williams, J. G. and Rhodes, M. D. : "Effect of Resin on the Impact Damage Tolerance of Graphite/Epoxy Laminates.", Composite Materials : Testing and Design (Sixth Conference), ASTM STP 787, Daniel, I. M. editor, ASTM, 1982, pp 450 - 480.

6. Gosse, J. H. and Mori, P. B. Y. : "Impact Damage Characterization of Graphite/Epoxy Laminates.", Proceedings of the American Society for Composites, Third Technical Conference, September 25 - 29, 1988, Seattle, Washington.

7. Guynn, E. G. and O'Brien, T. K. : "The Influence of Layup and Thickness on Composite Impact Damage and Compression Strength.", AIAA/ASCE/AHS 26th Structures, Structural Dynamics and Materials Conference, April 15 - 17, 1985, Orlando, Florida.

8. Masters, J. E. editor : "Fractography of Modern Engineering Materials : Composites and Metals.", ASTM STP 948, ASTM, 1987.

9. Lance, D. G. and Nettles, A. T. : "Low Velocity Instrumented Impact Testing of Four New Damage Tolerant Carbon/Epoxy Composite Systems.", NASA TP 3029, July 1990.

10. Chang, F. K., Choi, H. Y., and Jeng, S. T. : "Characterization of Impact Damage Tolerance in Laminated Composites.", SAMPE Journal, volume 26, number 1, January/February 1990 pp 18 - 25.

11. DeSisto, T. S. editor : "Instrumented Impact Testing.", ASTM STP 563, ASTM, 1974.

12. Nettles, A. T. : "Instrumented Impact and Residual Tensile Strength of Eight Ply Carbon/Epoxy Specimens.", NASA TP 2981, January, 1990.

13. Portanova, M. A., Poe, C. C. Jr., and Whitcomb, J. D. : "Open Hole and Post Impact Compression Fatigue of Stitched and Unstitched Carbon/Epoxy Laminates.", NASA TM 102676, June 1990.

14. Williams, J. G., O'Brien, T. K., and Chapman, A. J. : "Comparison of Toughened Composite Laminates using NASA Standard Damage Tolerance Tests.", ACEE Composite Structures Technical Conference, Seattle, Washington, August 13 - 15, 1984.

15. Rotem, A. : "Residual Flexural Strength of FRP Composites Subject to Transverse Impact Loading.", SAMPE Journal, volume 24, number 2, March/April 1988, pp 19-25.

16. Aleska, J. C. : "Low Energy Impact Behavior of Composite Panels.", Journal of Testing and Evaluation, volume 6, number 3, May 1978, pp 202-210.

17. Winkel, J. D. and Adams, D. F. : "Instrumented Drop Weight Impact Tests of Crossply and Fabric Composites.", Composites, volume 16, number 4, October 1985, pp 268-278.

18. Cantwell, J. J., Curtis, P. T., and Morton, J. : "An Assessment of Impact Performance of DFRP Reinforced with High Strain Carbon Fibers.", Composite Science and Technology, volume 25, number 2, 1986, pp 133-148.

19. Husman, G. E., Whitney, J. M., and Halpin, J. C. : "Residual Strength Characteristics of Laminates Subject to Impact Loading.", "Foreign Object Impact Damage to Composites", ASTM STP 568, 1975, pp 92 - 113.

20. Verpoest, I., Marien, J., Devos, J., and Weavers, J. : "Absorbed Energy, Damage and Residual Strength after Impact of Composite Laminates.", 6th International Conference on Composite Materials, Mathews, F. L., Buskell, N. C. R., Hodkinson, J. M., and Morton, J. editors, Elsevier Applied Science Publishers, NY, 1985, p 3.485.
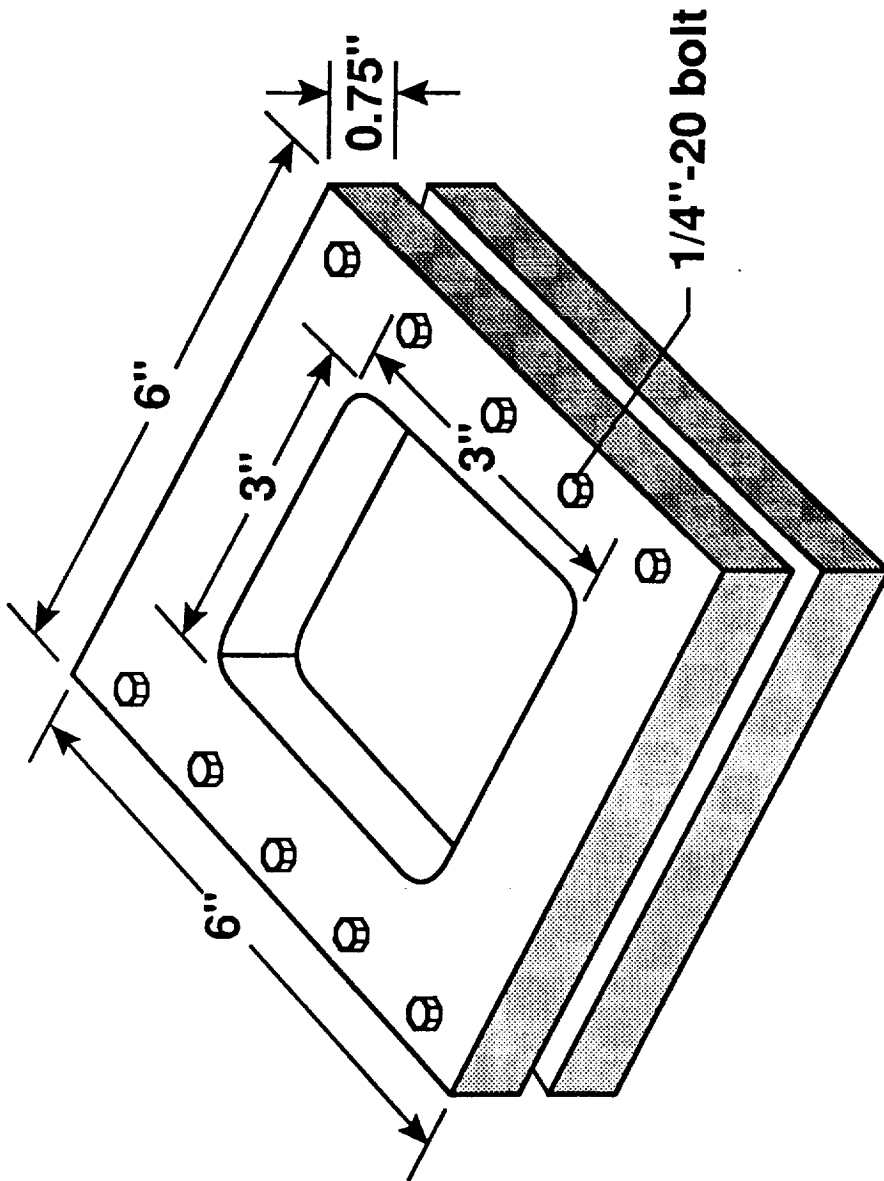
Figure 1. Impact fixture
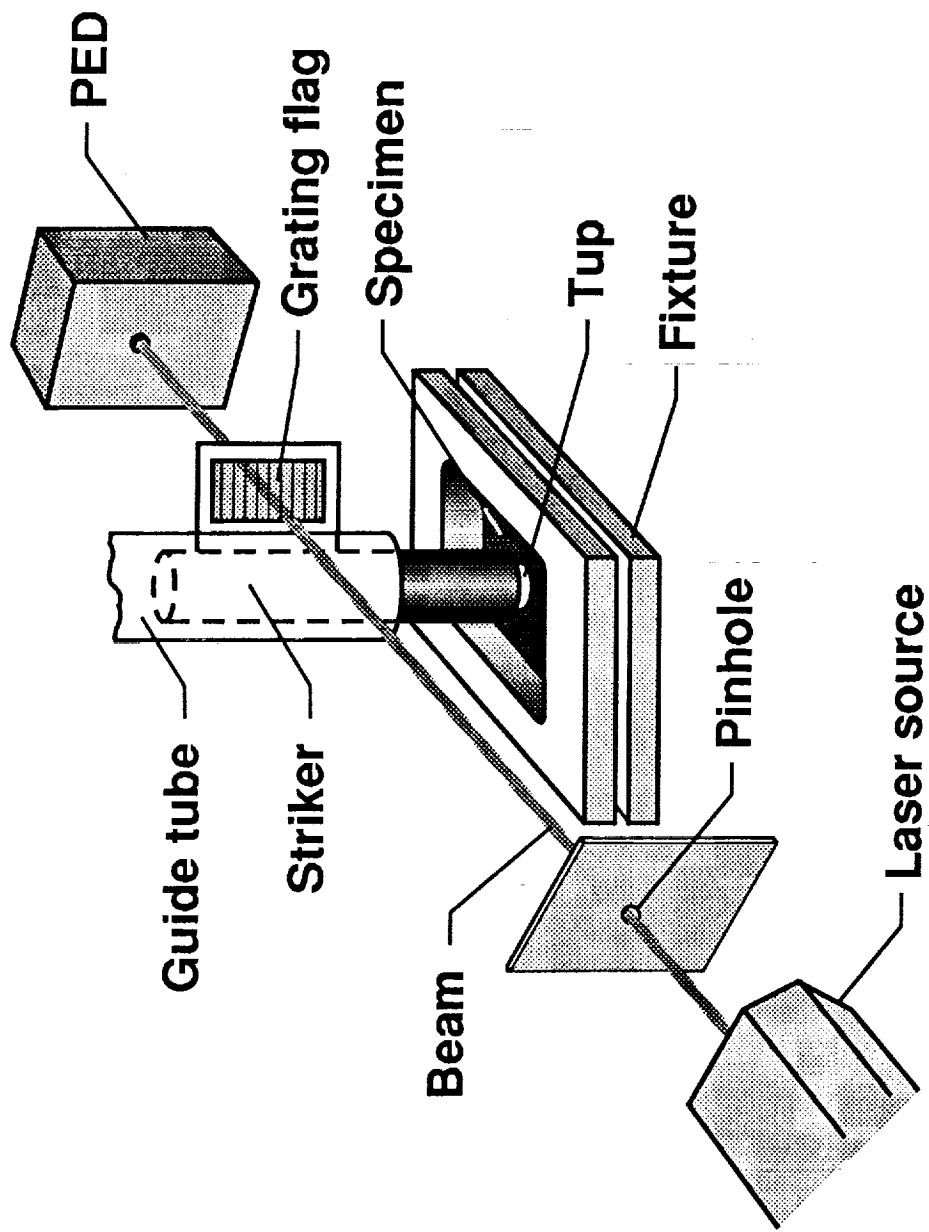
Figure 2. Schematic of impact test
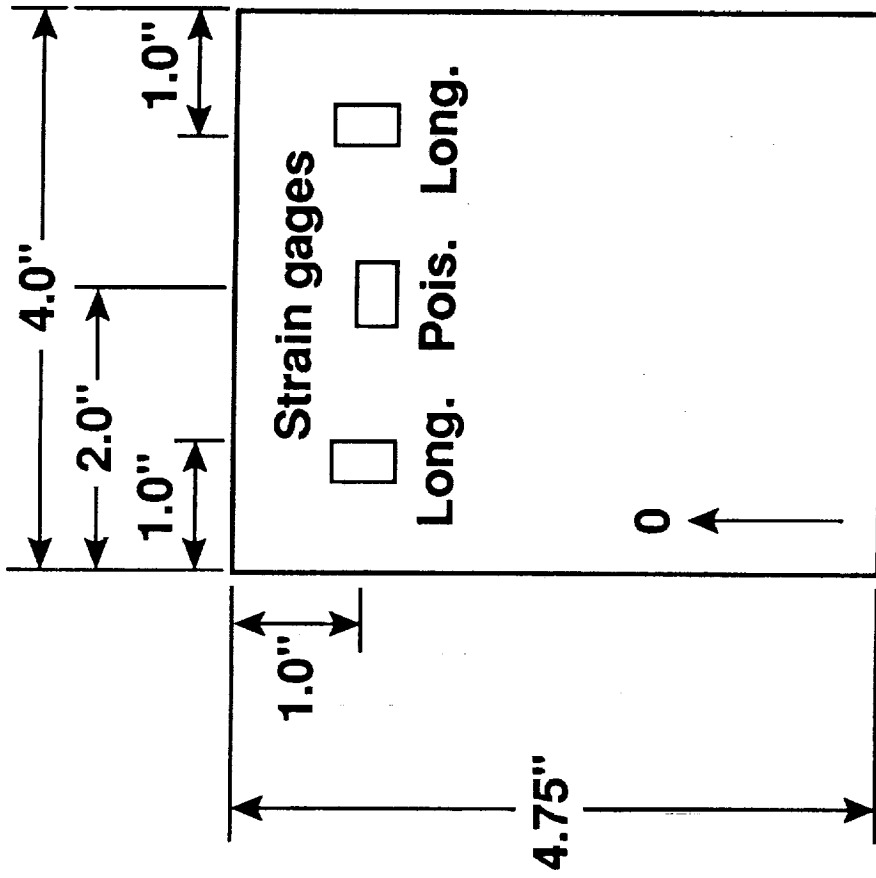
Figure 3. Schematic of compression specimen.
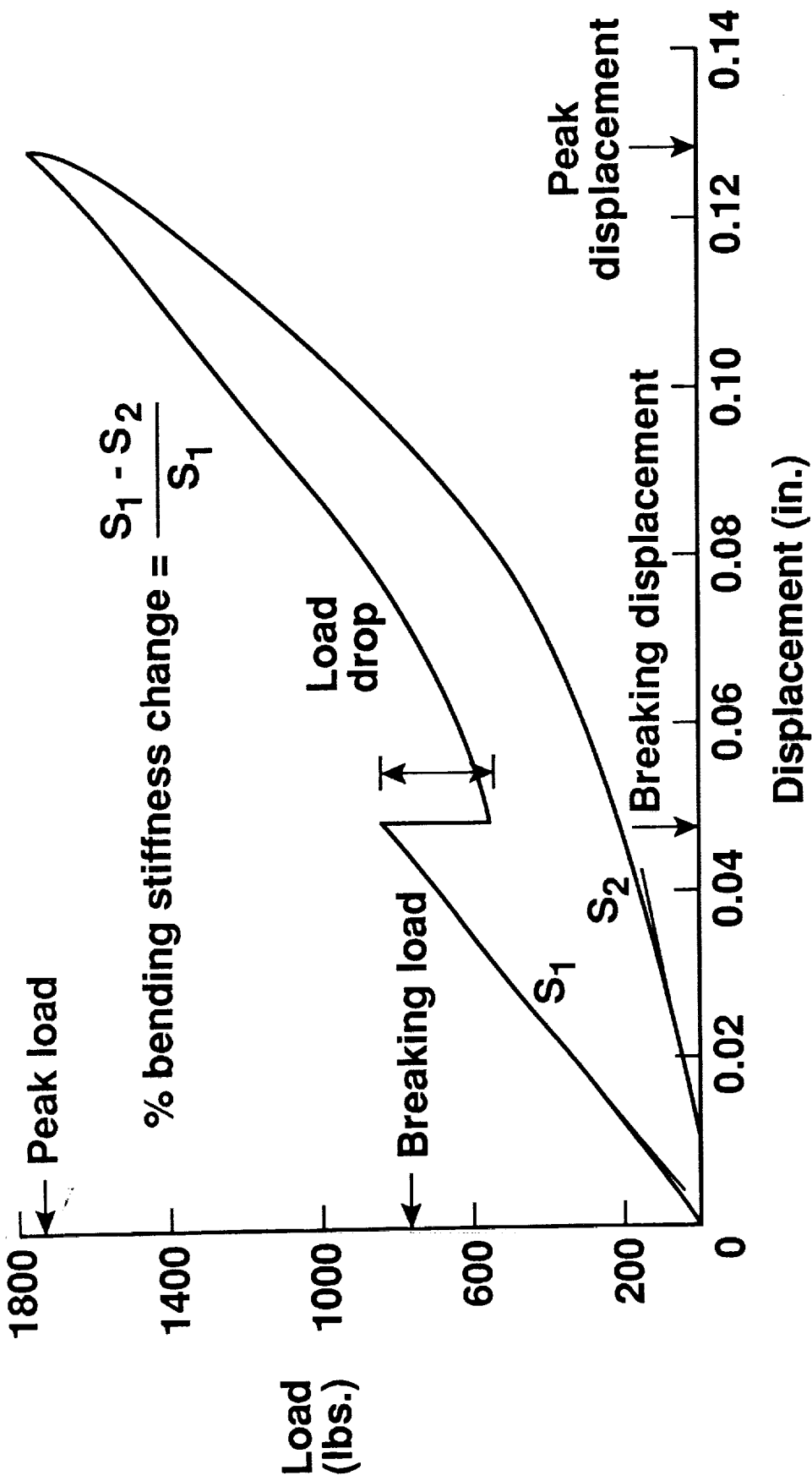
Figure 4. Typical impact load-displacement curve.

$$\% \text{ bending stiffness change} = \frac{S_1 - S_2}{S_1}$$

18
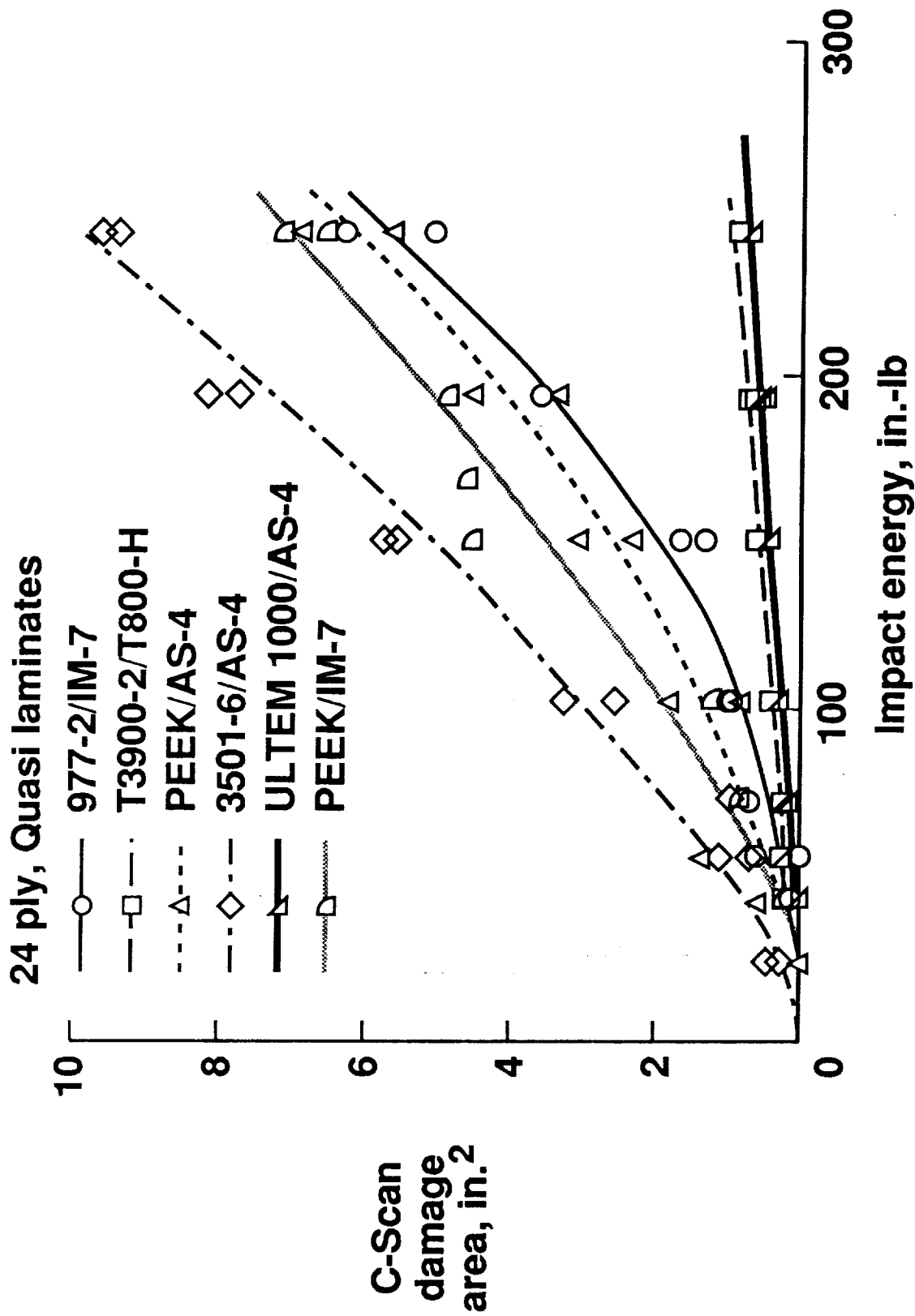
Figure 5. Impact damage area versus impact energy.
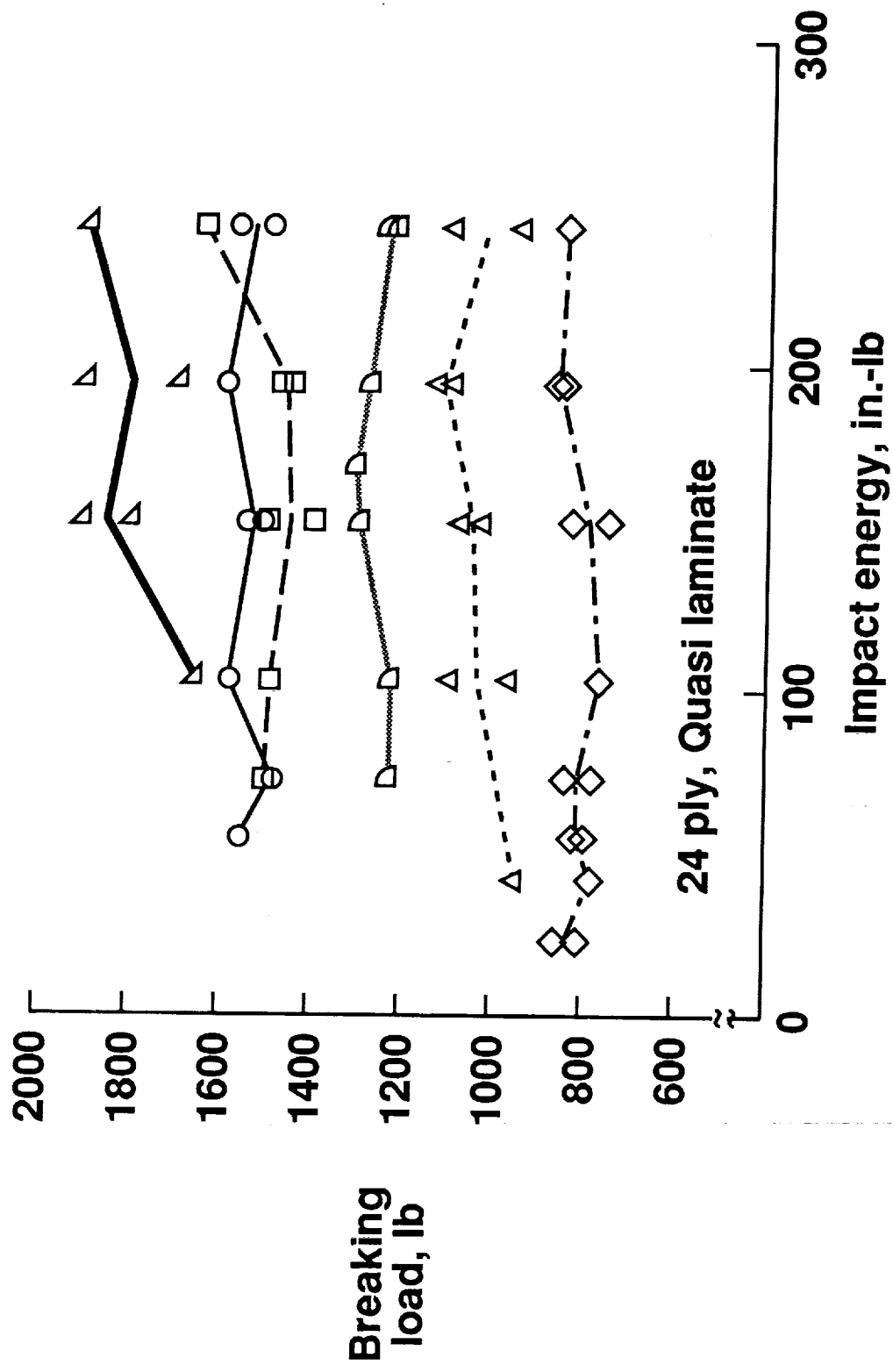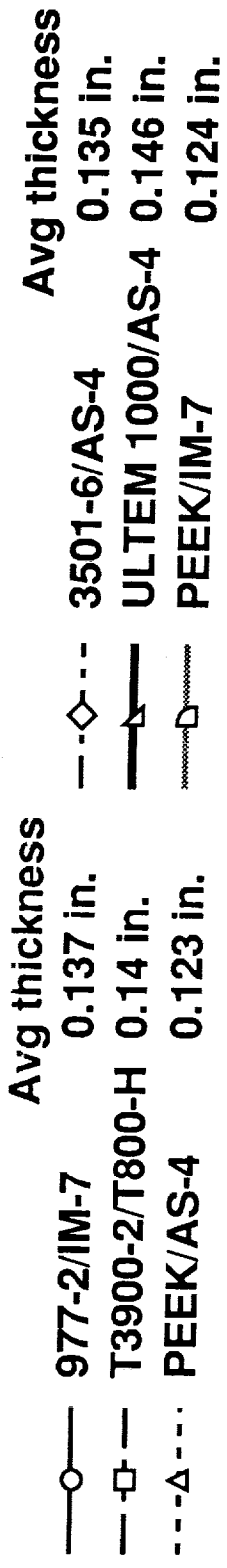
Figure 6. Breaking load versus impact energy.
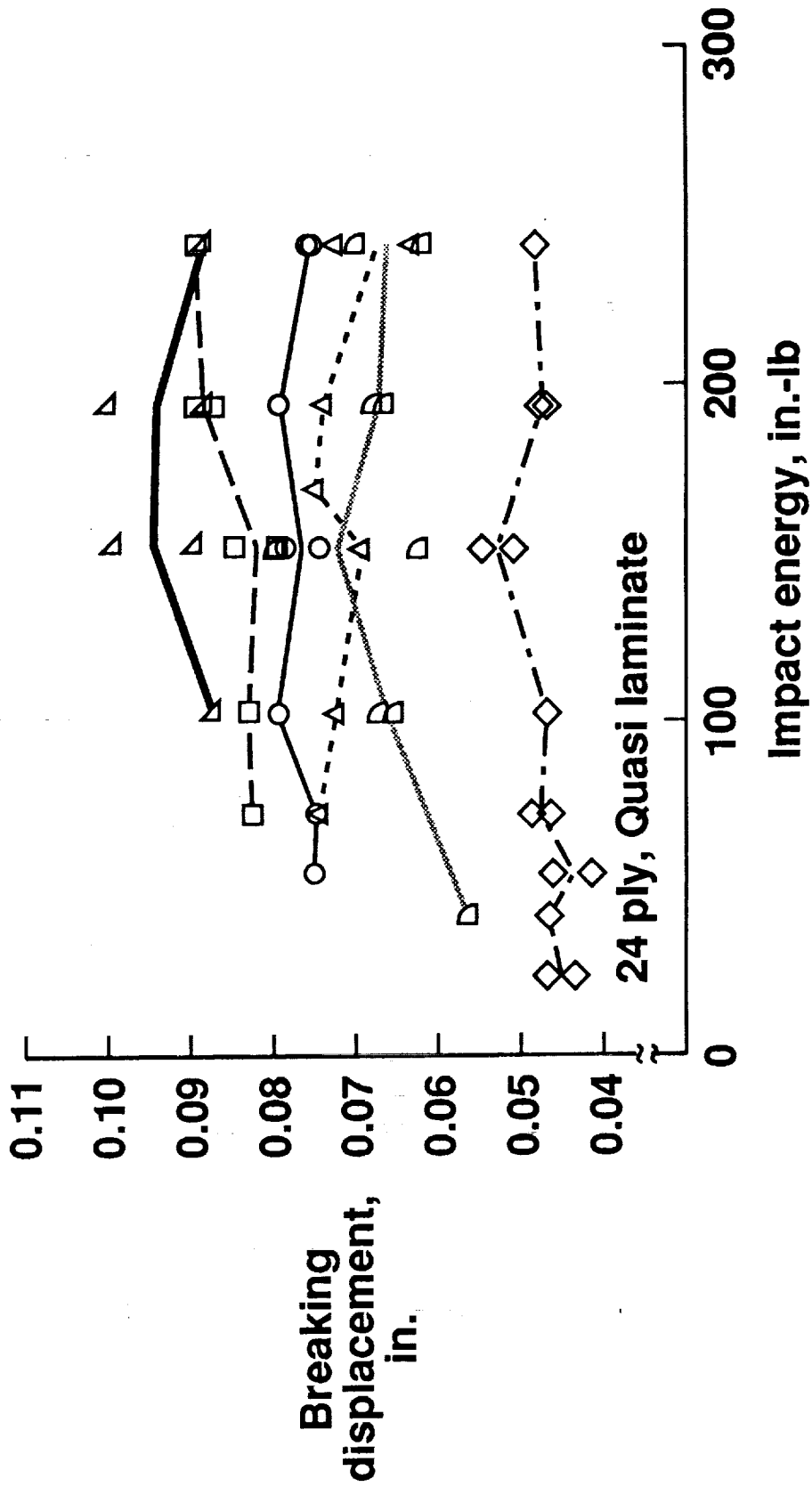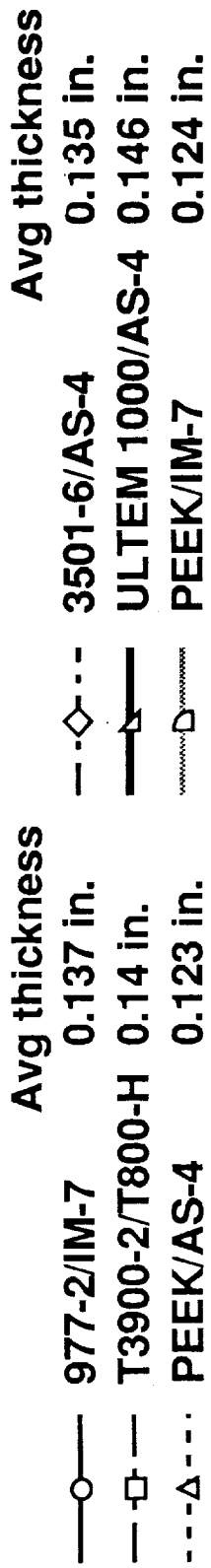
Figure 7. Breaking displacement versus impact energy.
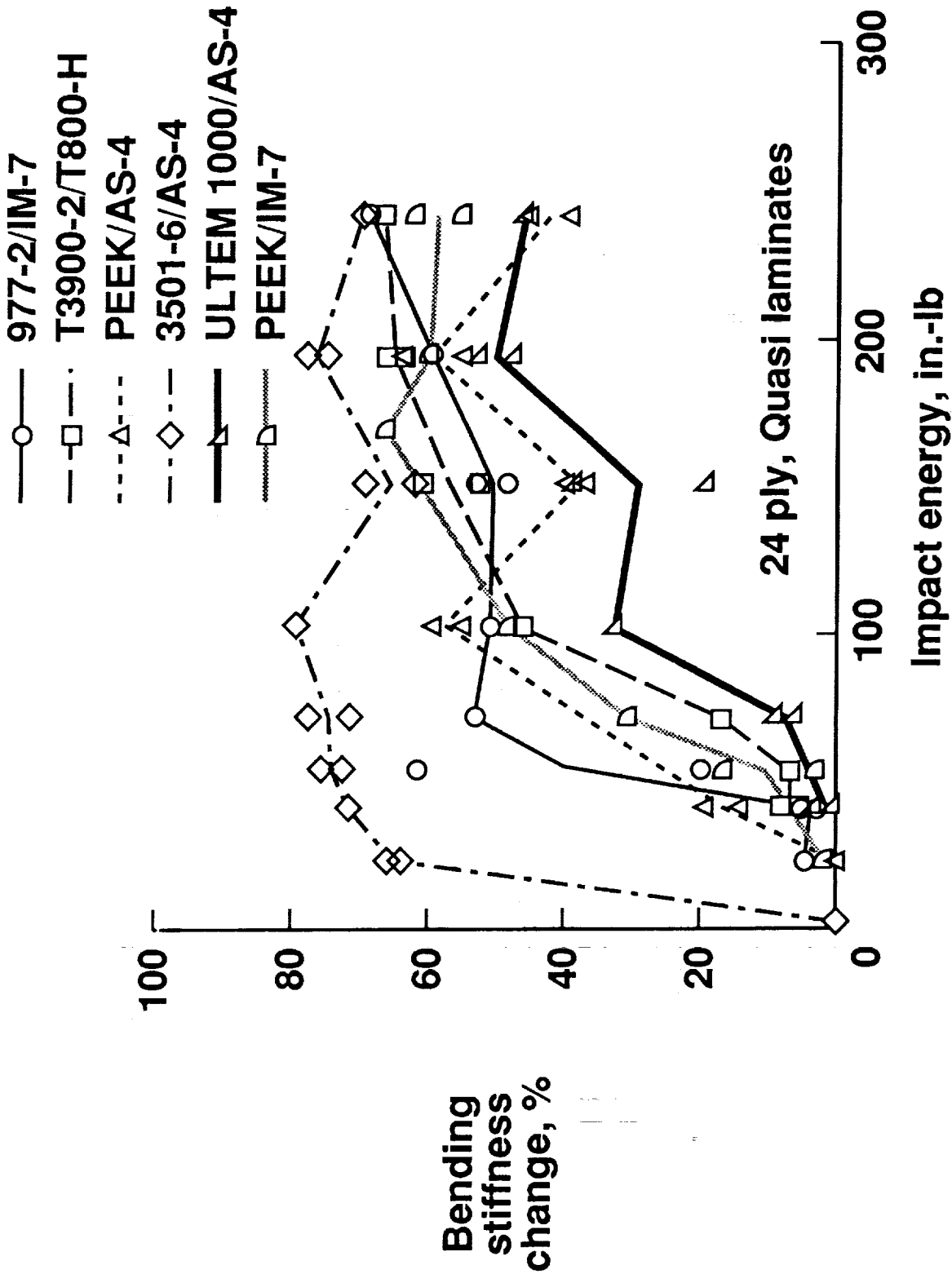
Figure 8. Change in bending stiffness versus impact energy.
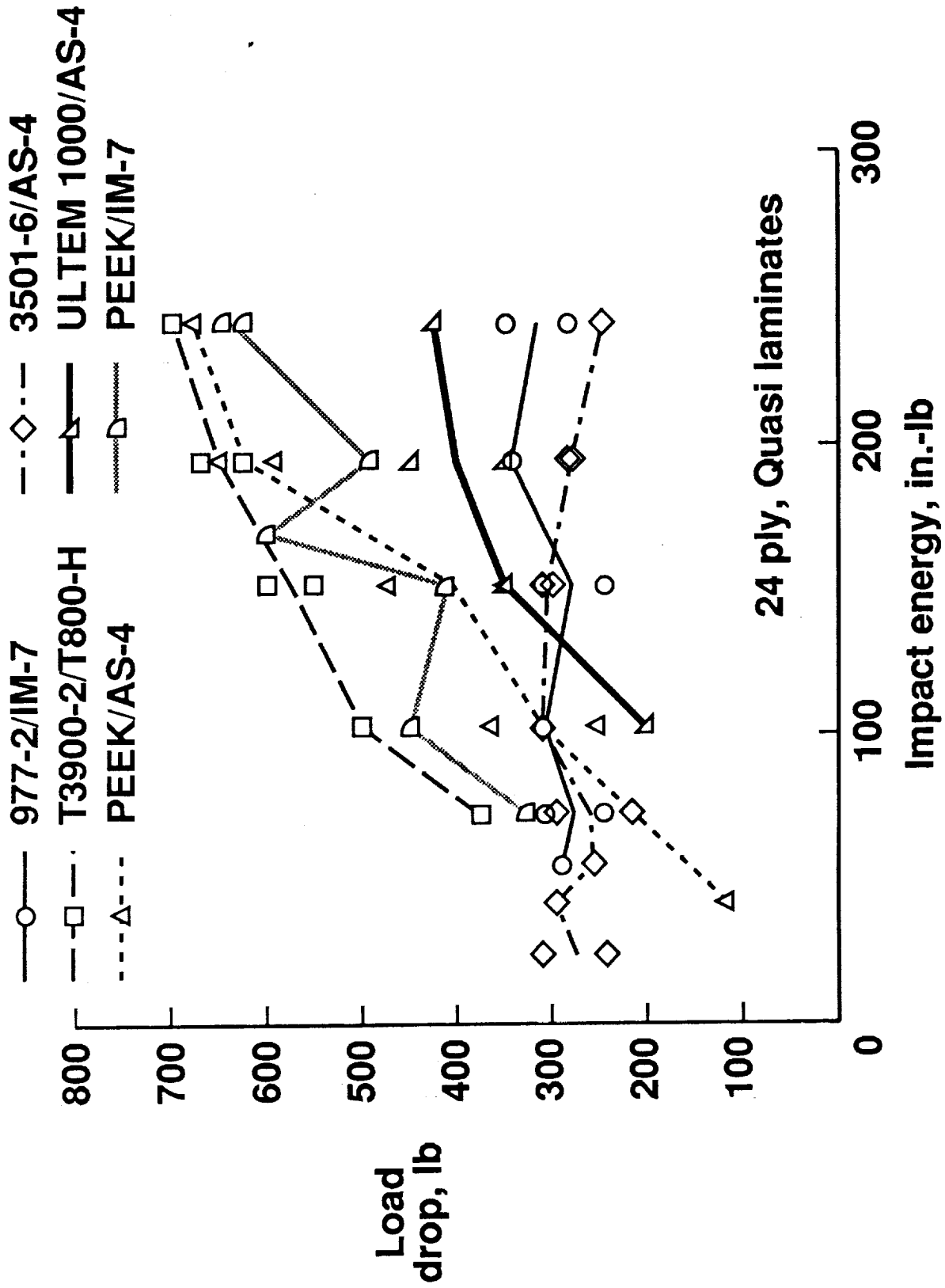
Figure 9. Load drop at break versus impact energy.
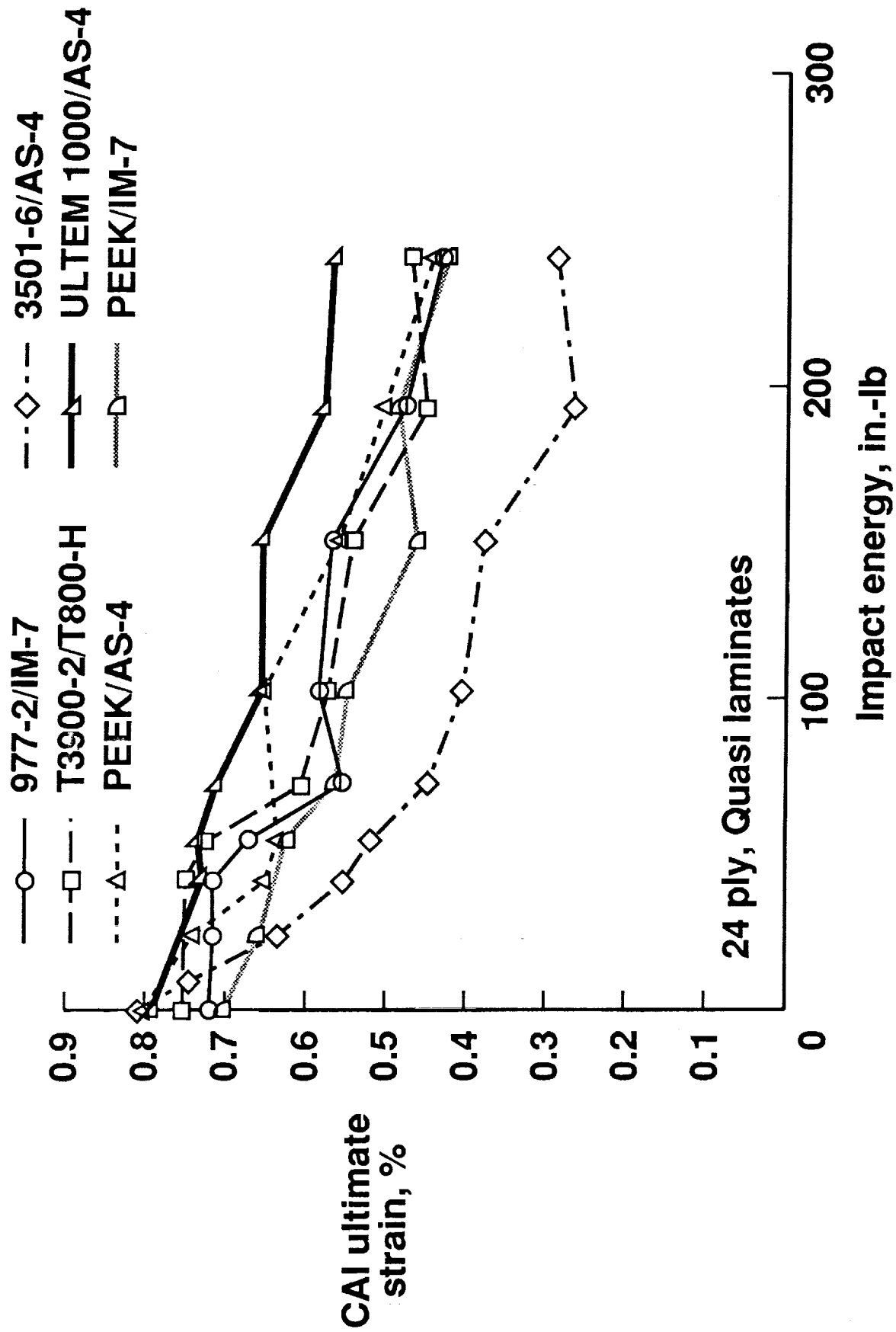
Figure 10. Post-impact compression strain versus impact energy.
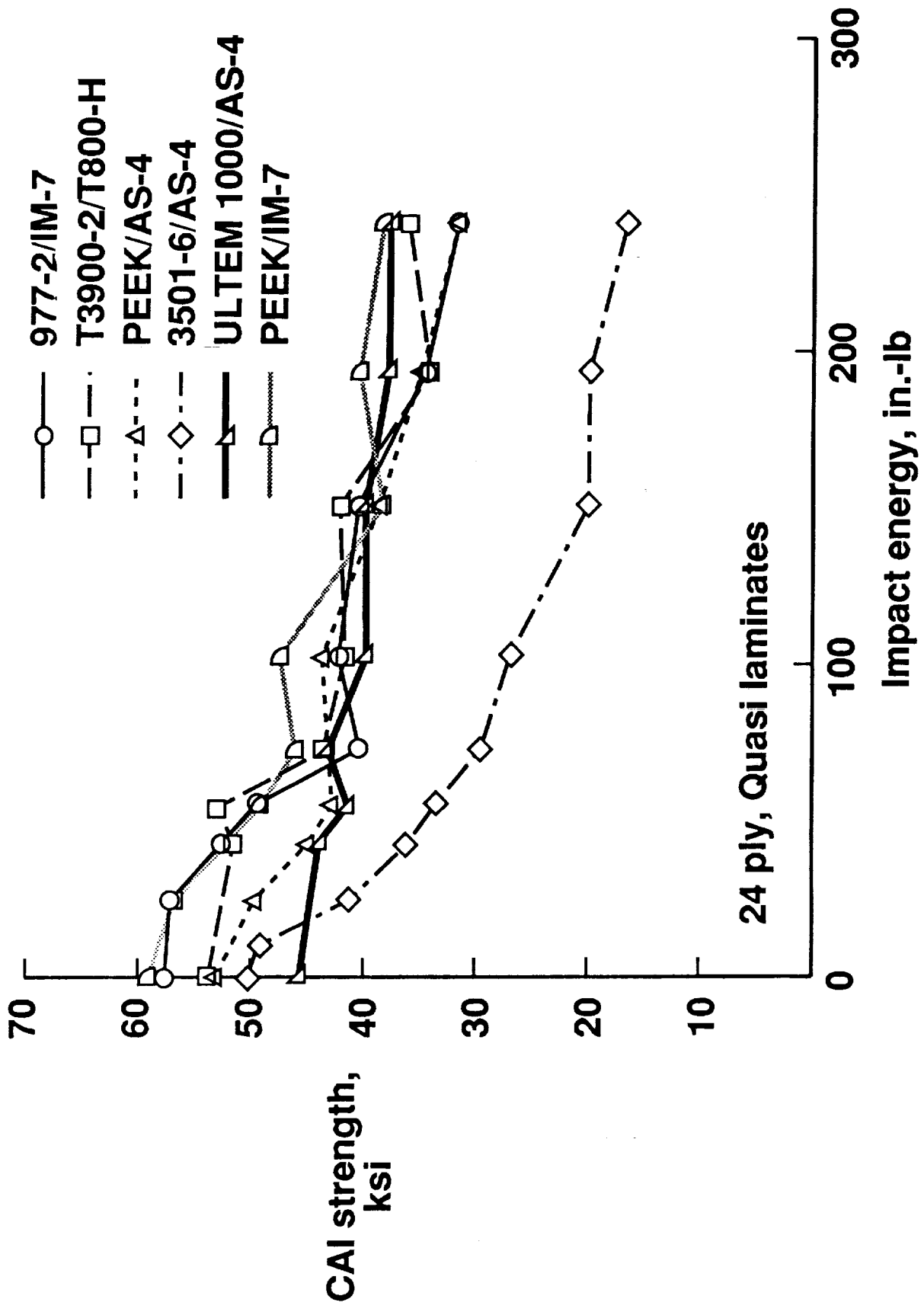
Figure 11. Post-impact compression strength versus impact energy.
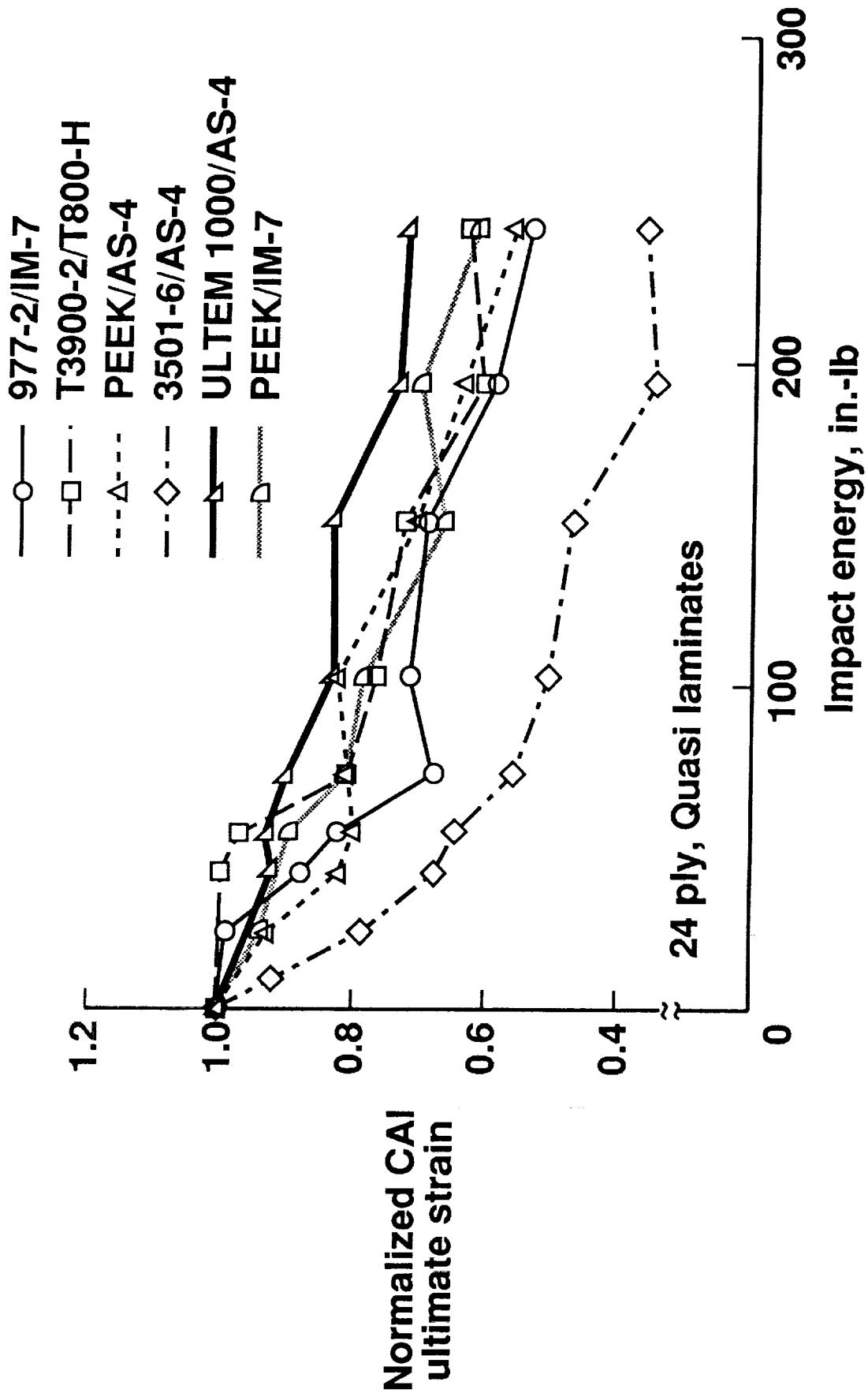
Figure 12. Normalized CAI strain versus impact energy.
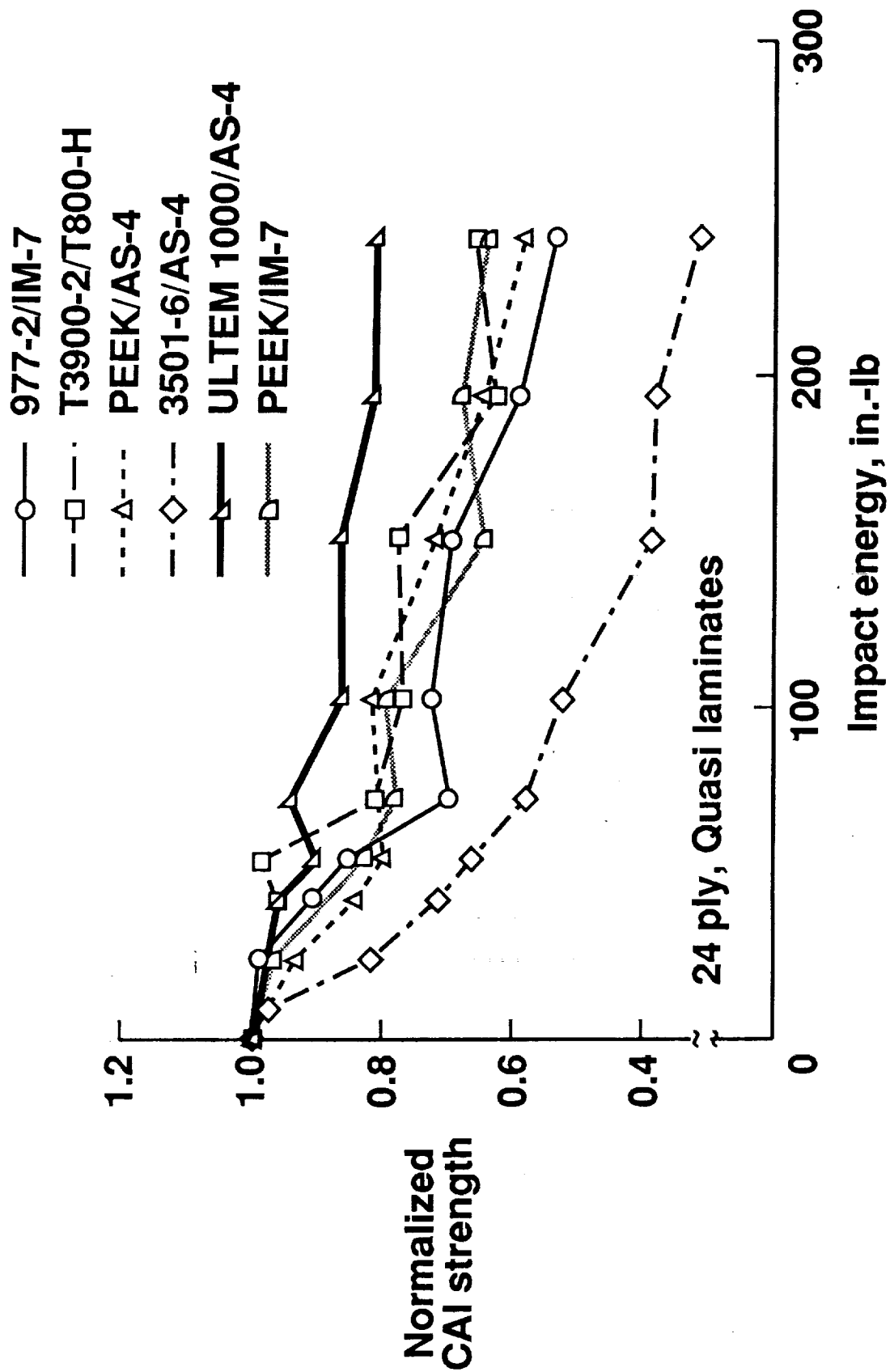
Figure 13. Normalized CAI strength versus impact energy.
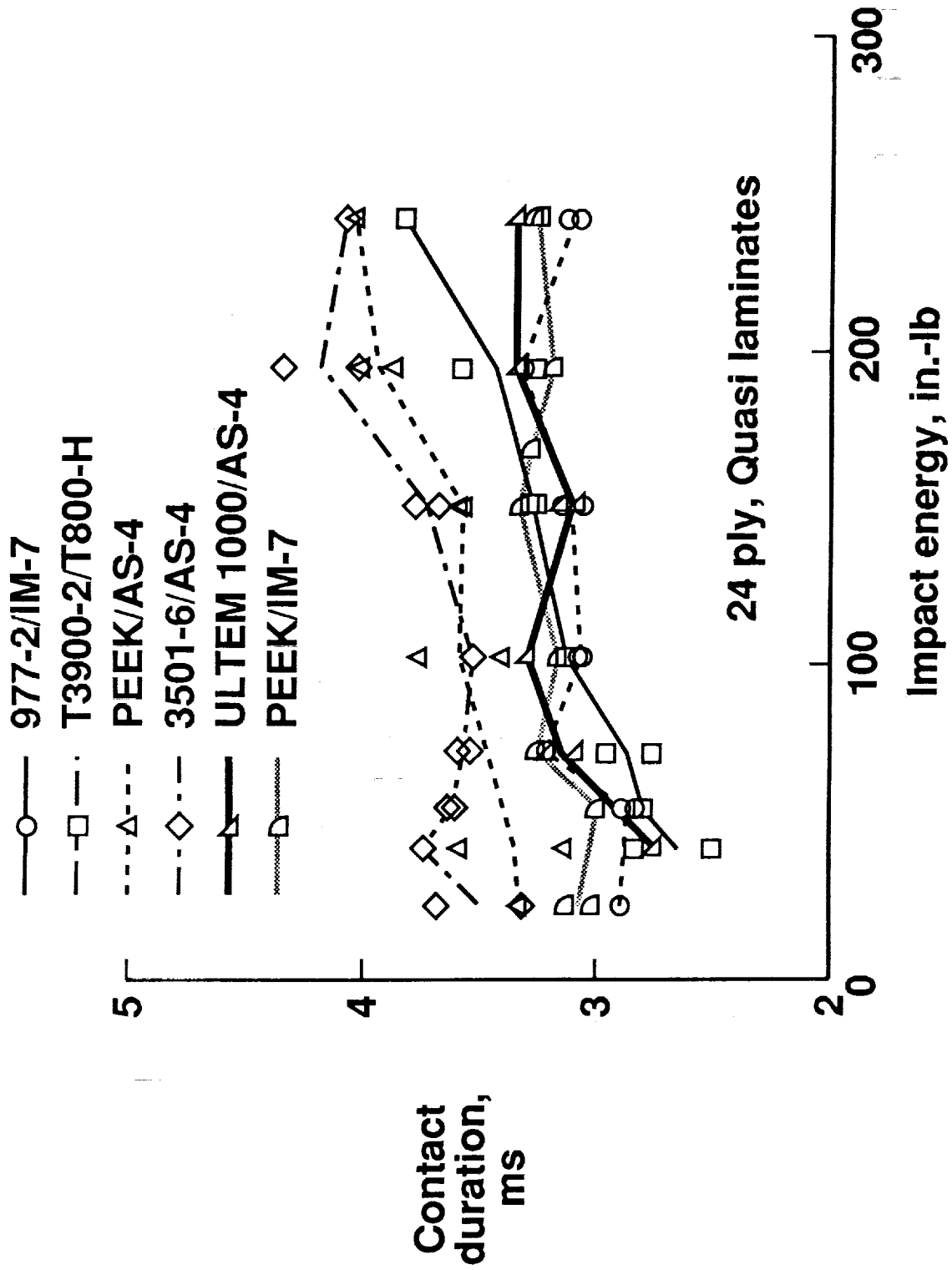
Figure 14. Contact duration versus impact energy.

28
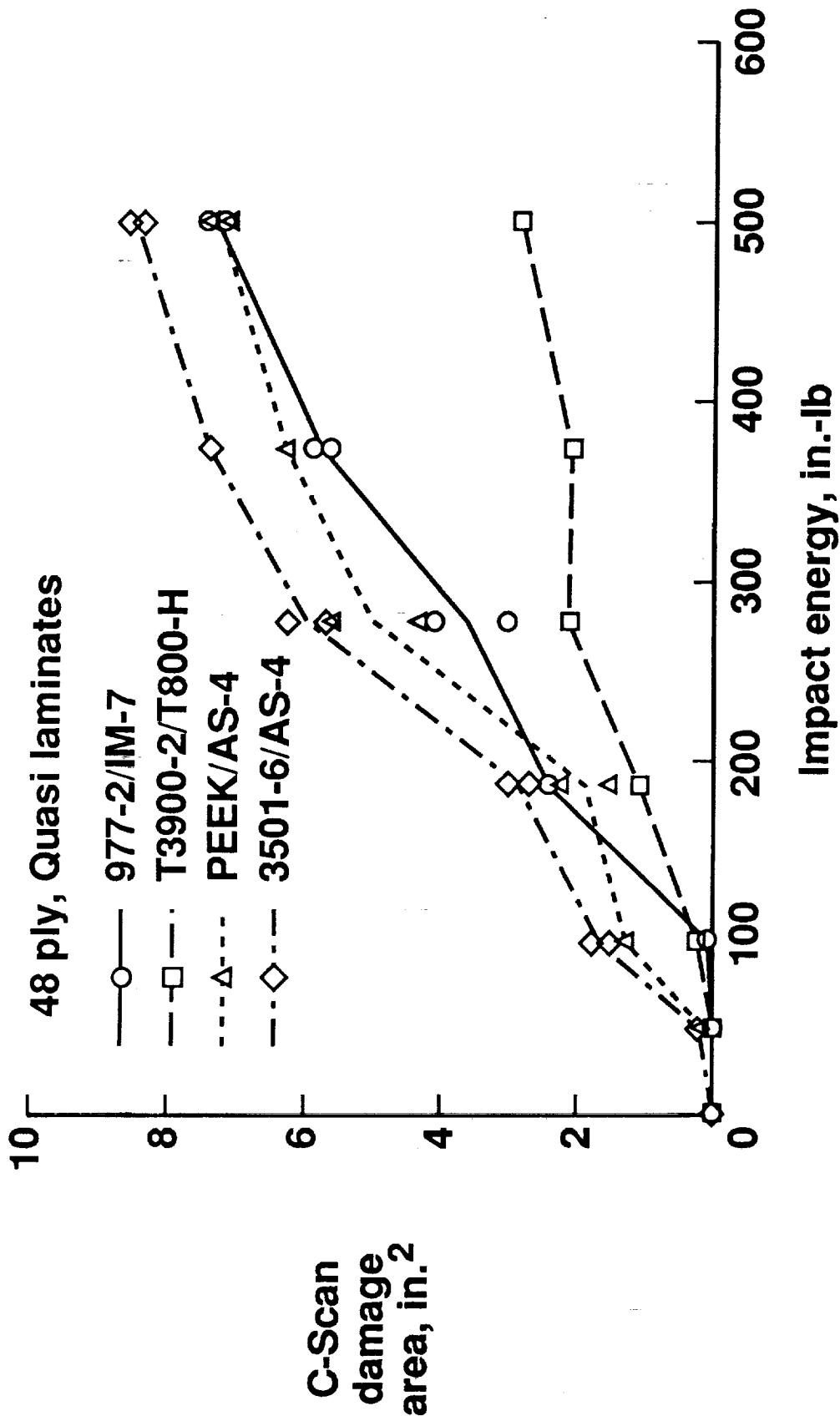
Figure 15. Damage areas of 48-ply laminates versus impact energy.
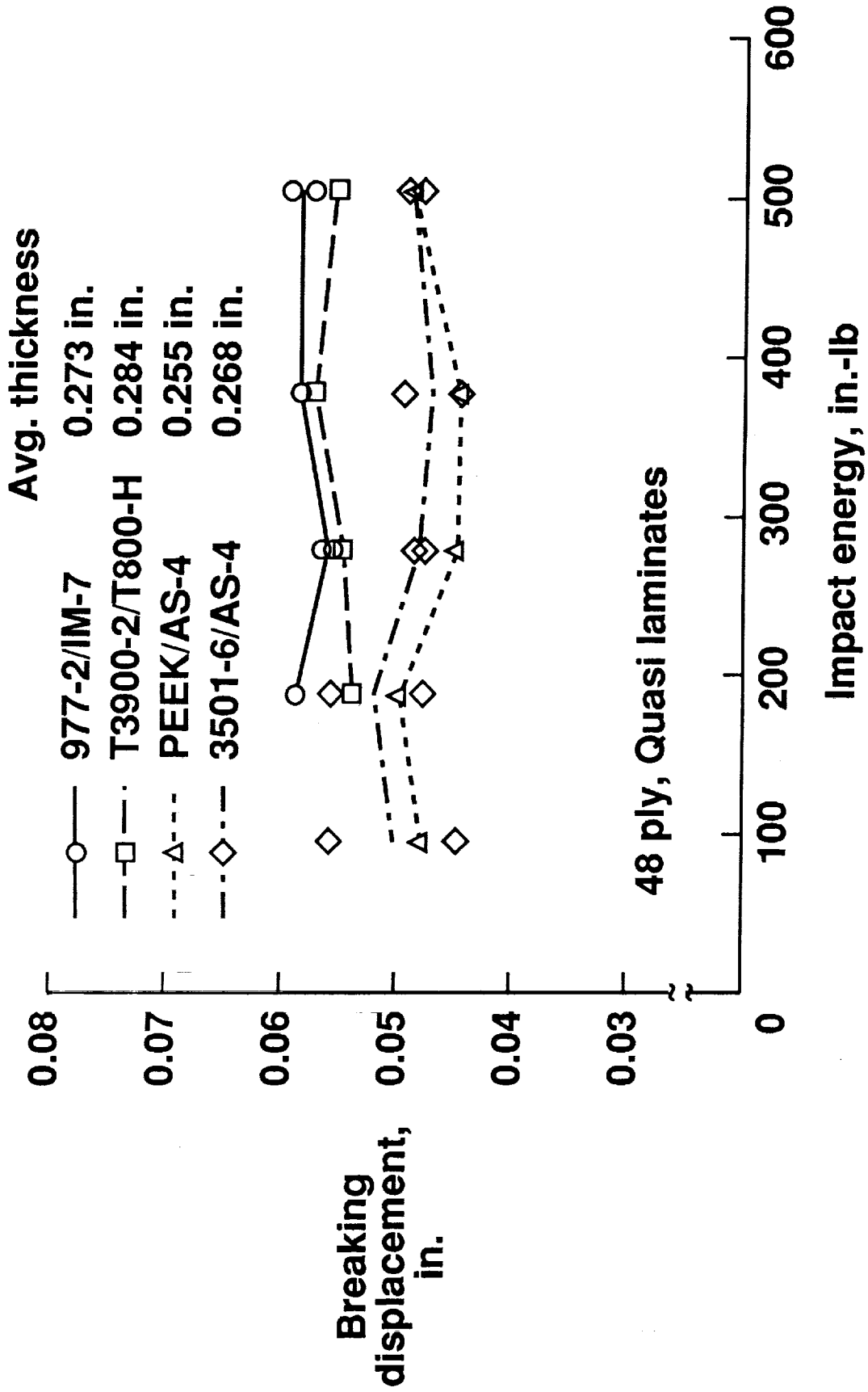
Figure 16. Breaking displacement of 48-ply laminates versus impact energy.
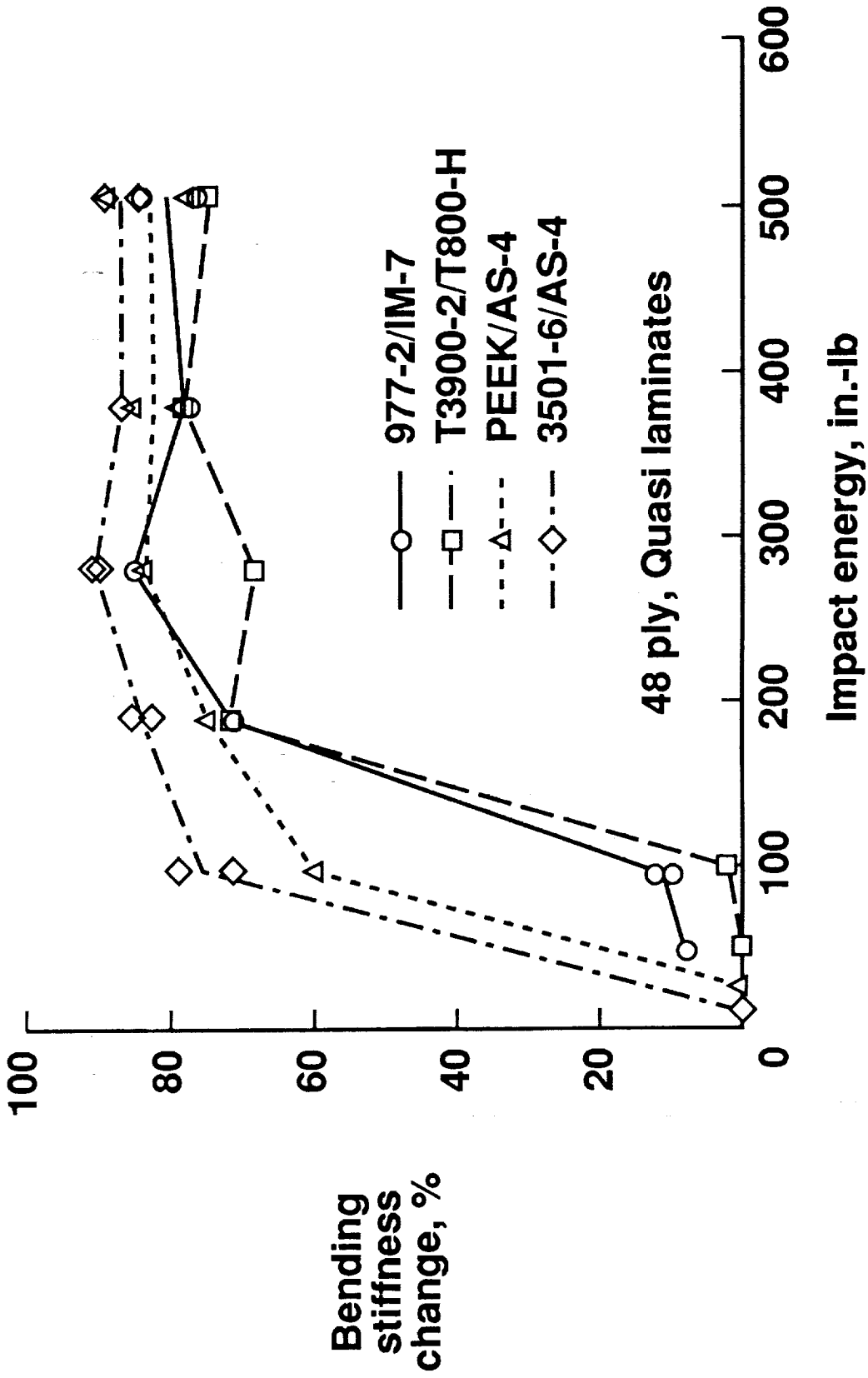
Figure 17. Change in bending stiffness of 48-ply laminates versus impact energy.
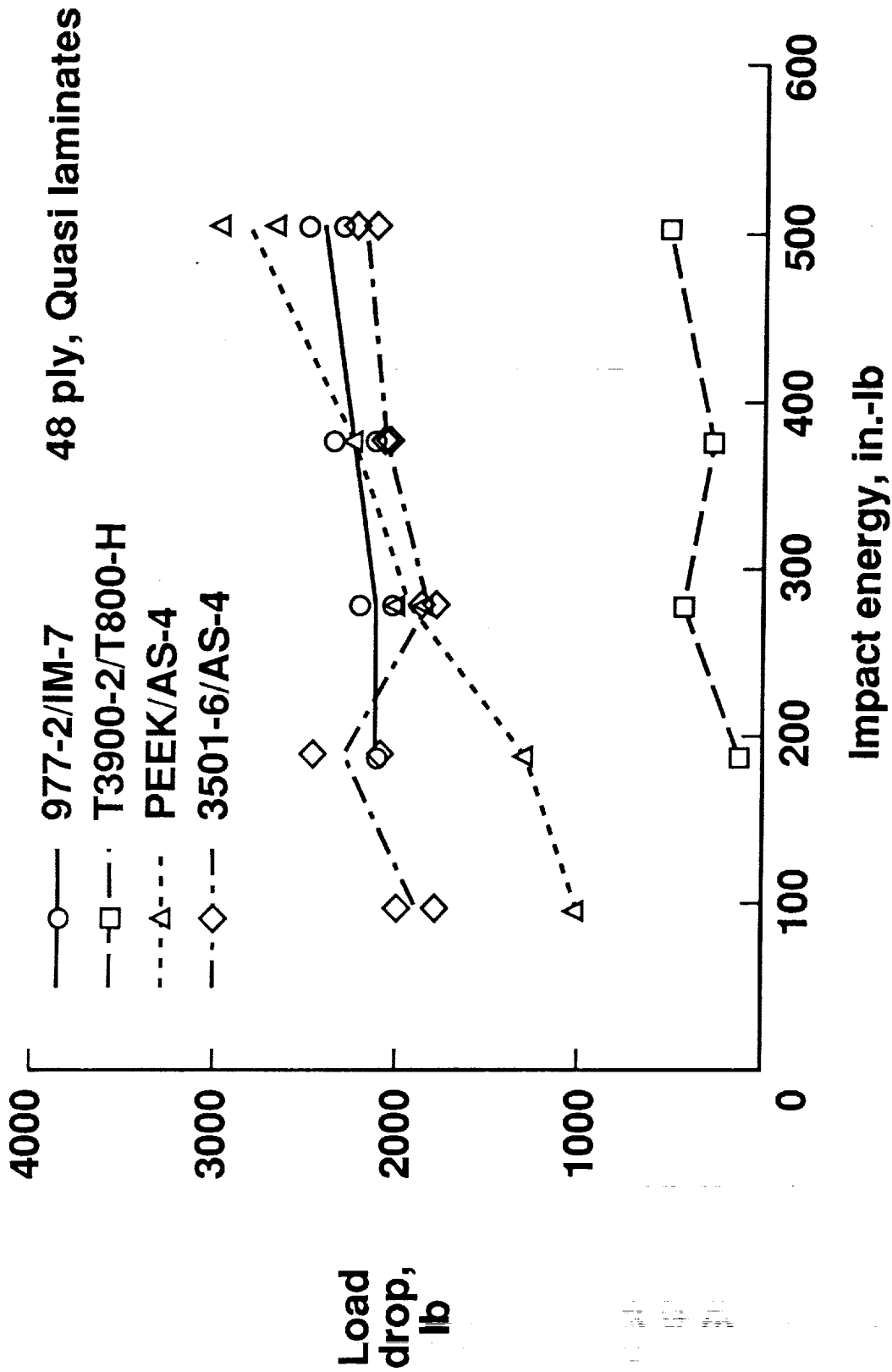
Figure 18. Load drops of 48-ply laminates versus impact energy.
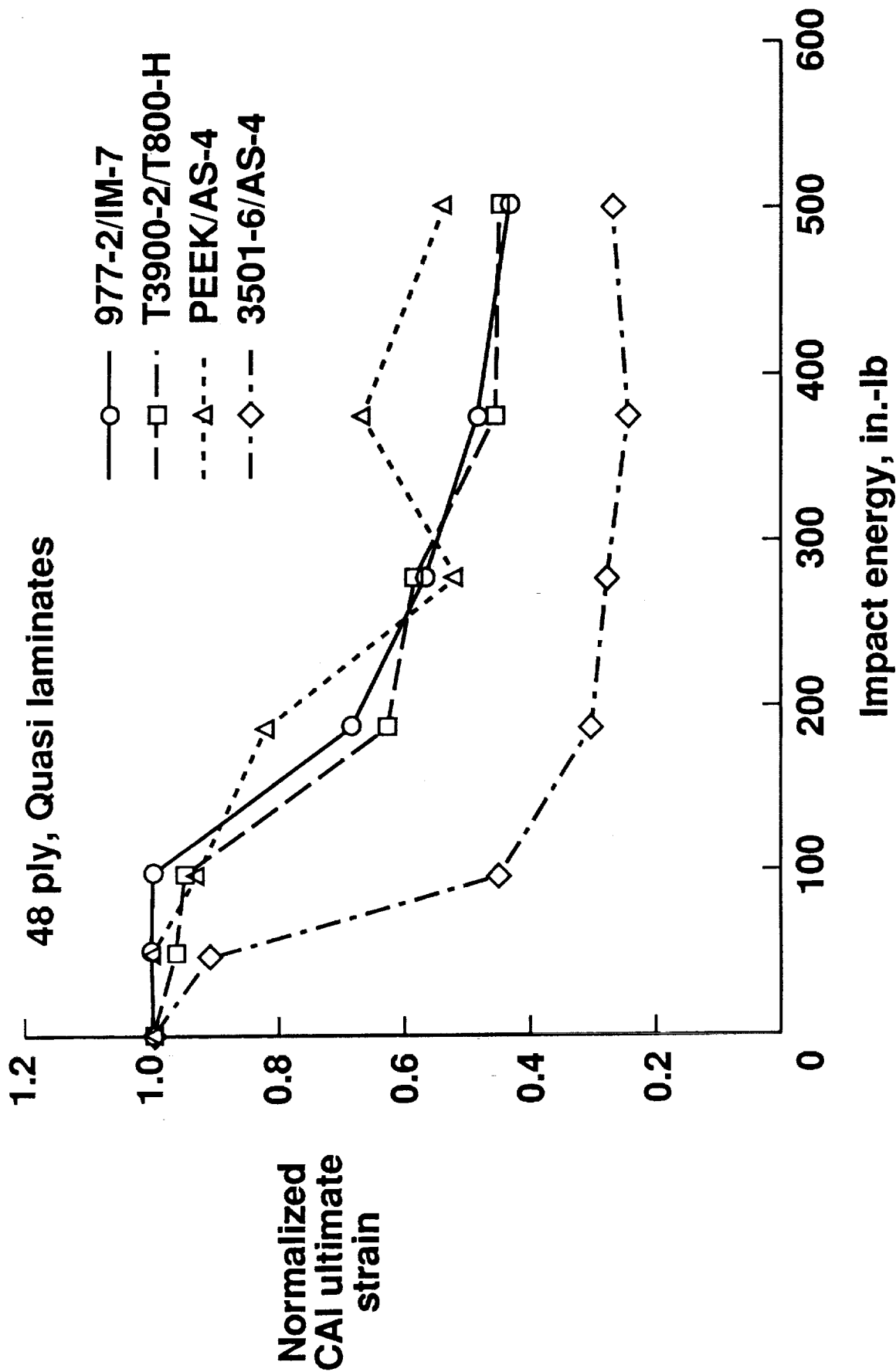
Figure 19. Normalized CAI strain versus impact energy (48-ply laminates).
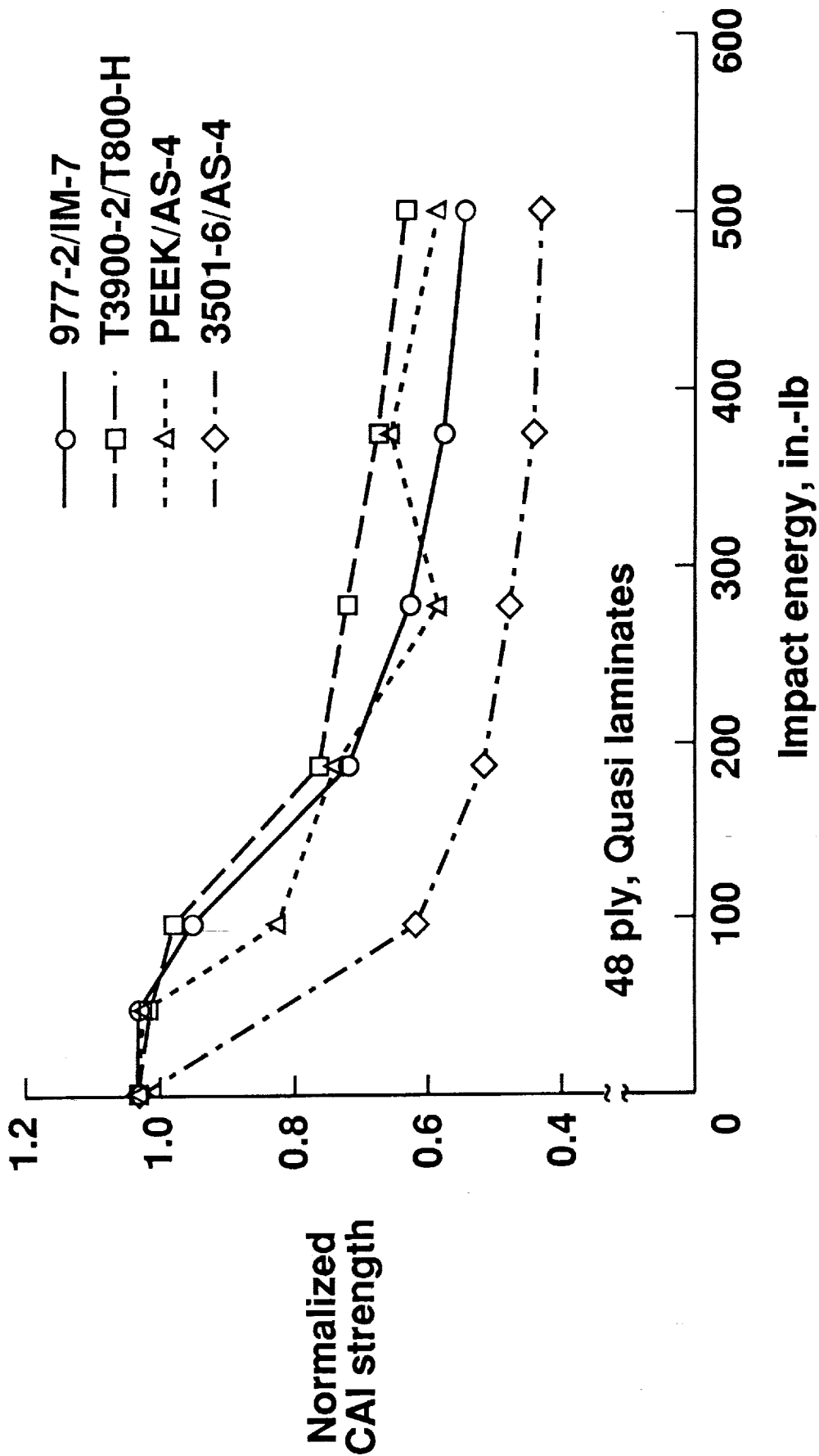
Figure 20. Normalized CAI strength versus impact energy (48-ply laminates).
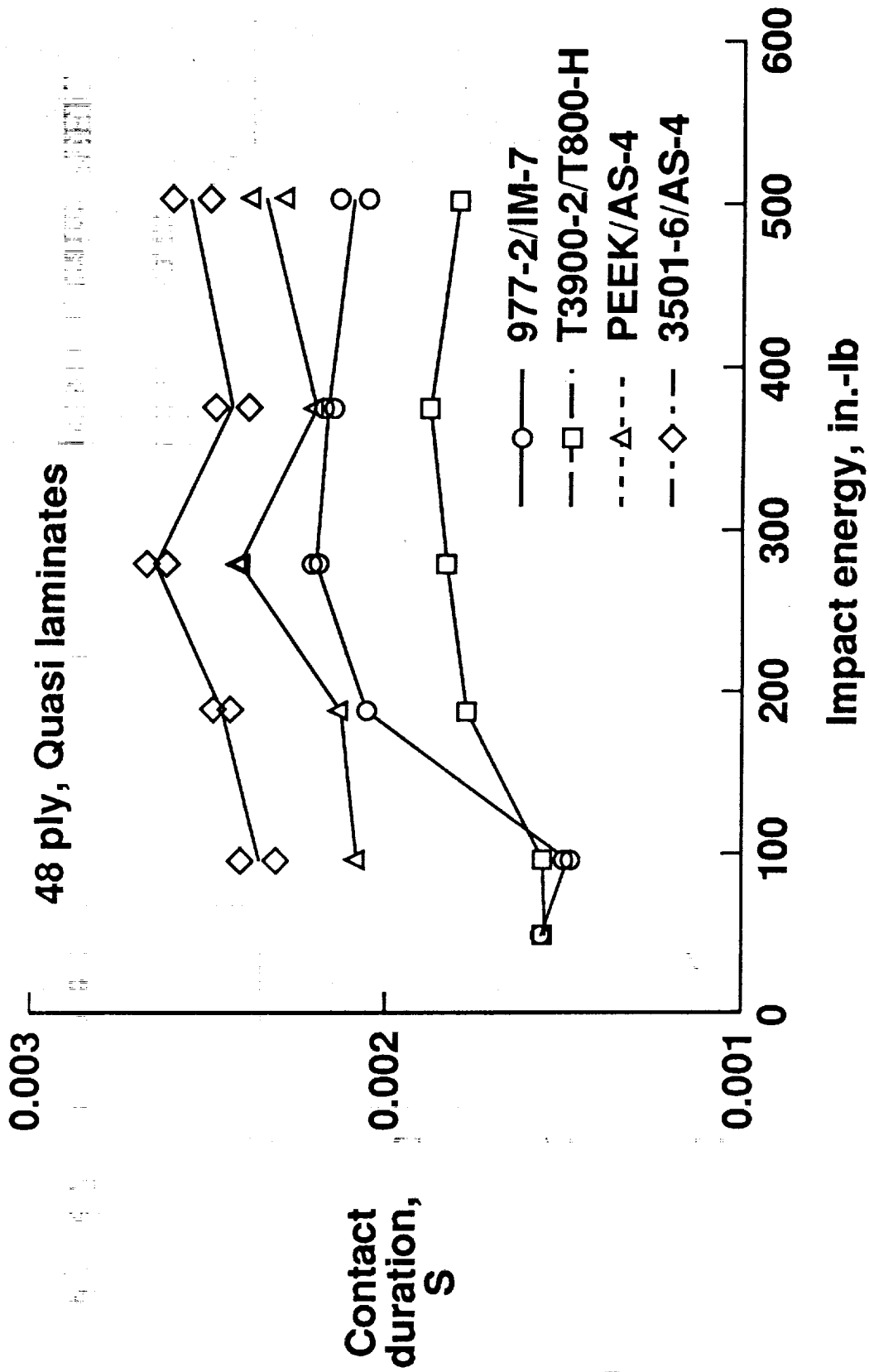
Figure 21. Contact duration versus impact energy (48-ply laminates).
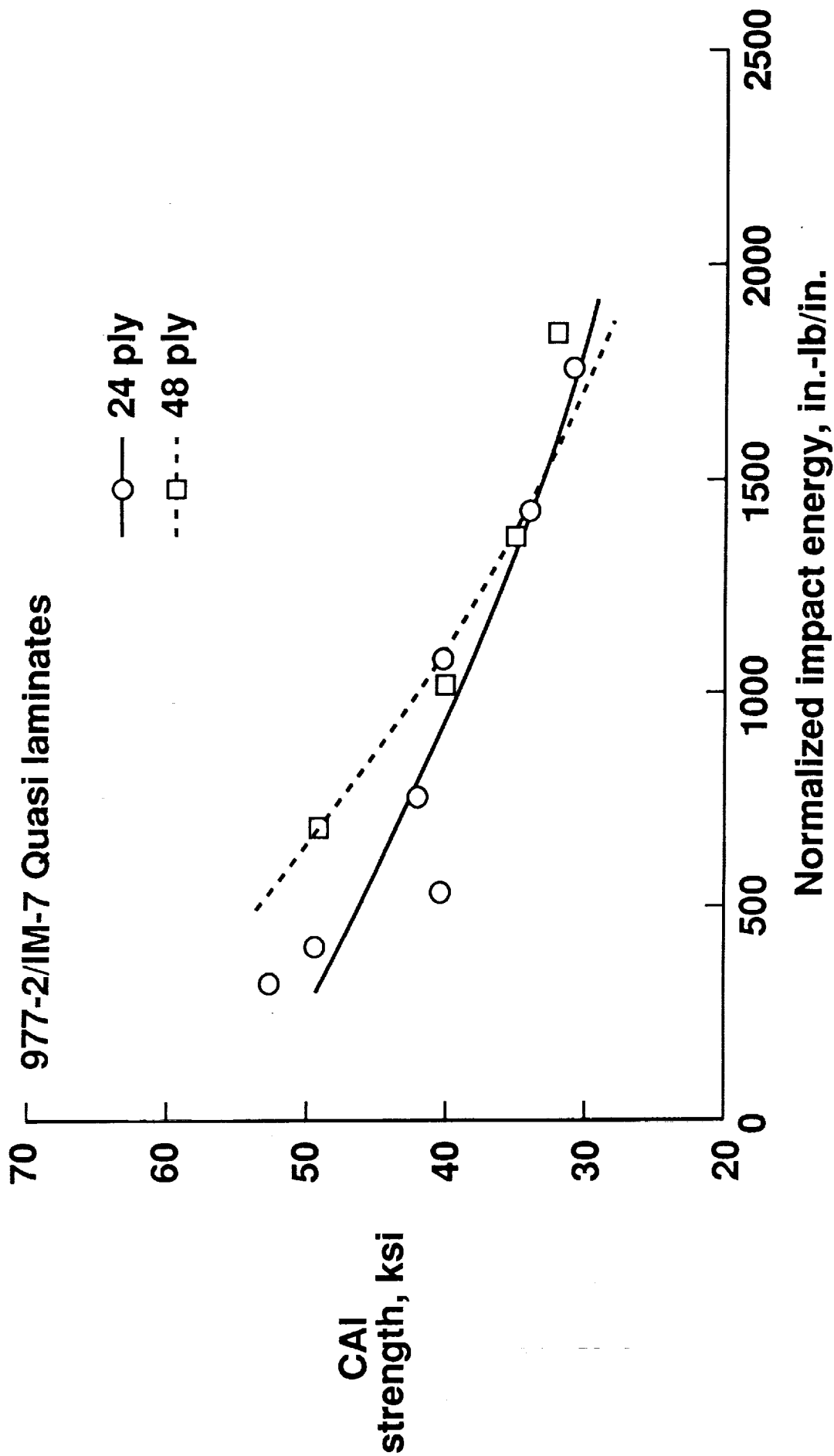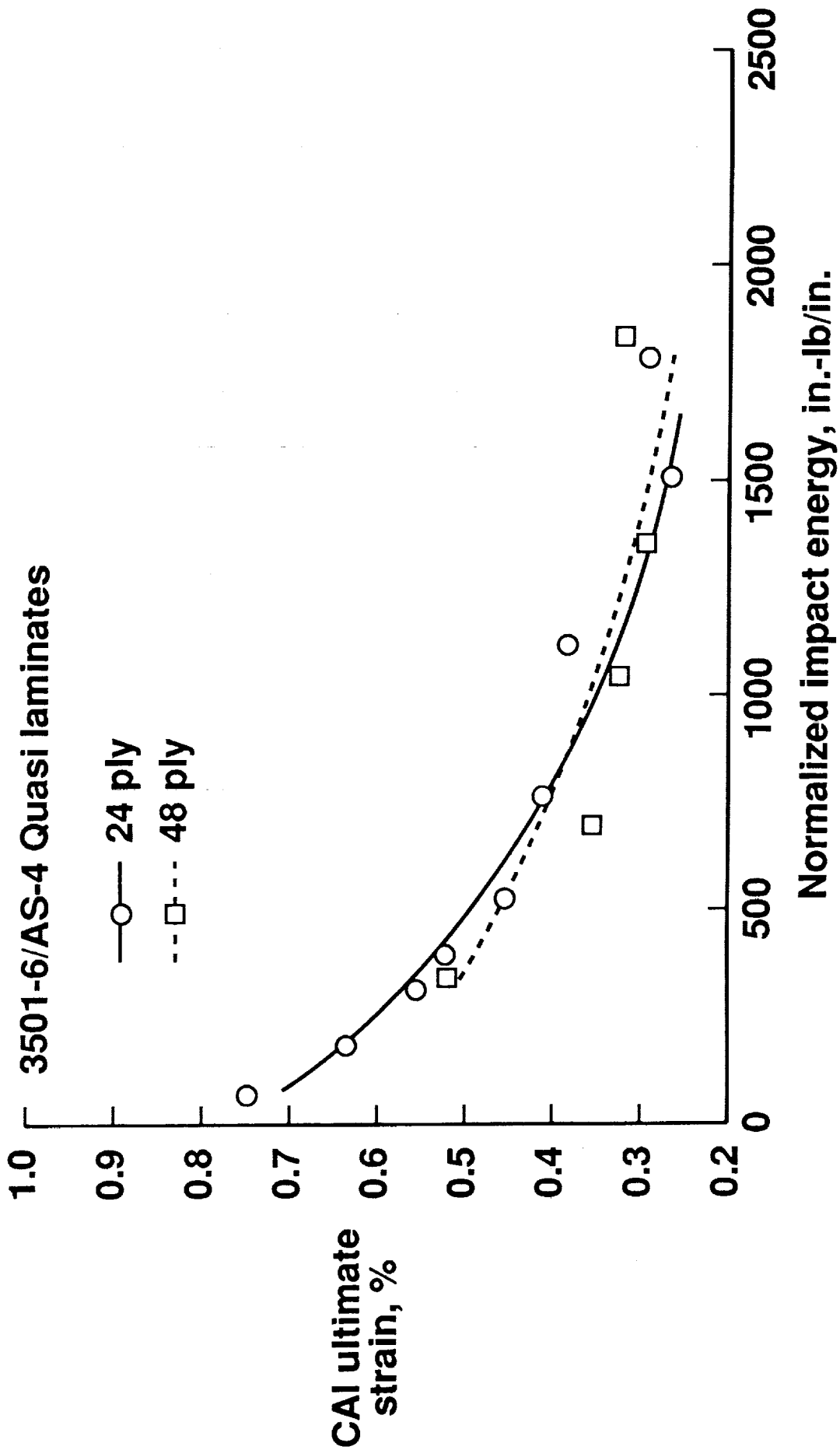
Figure 22. Influence of thickness on post-impact compression strain: PEEK.
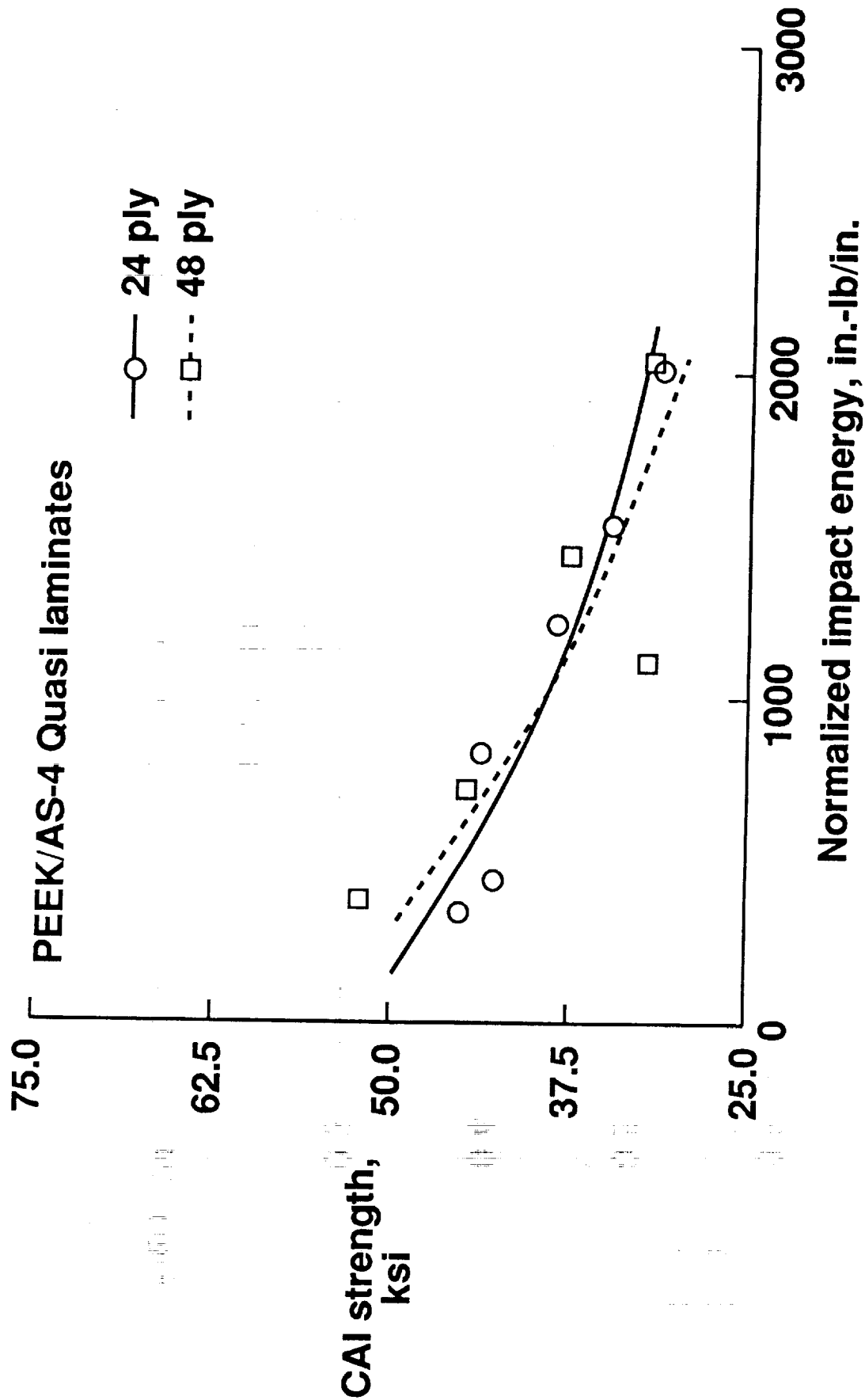
Figure 23. Influence of thickness on post-impact compression strength: PEEK.
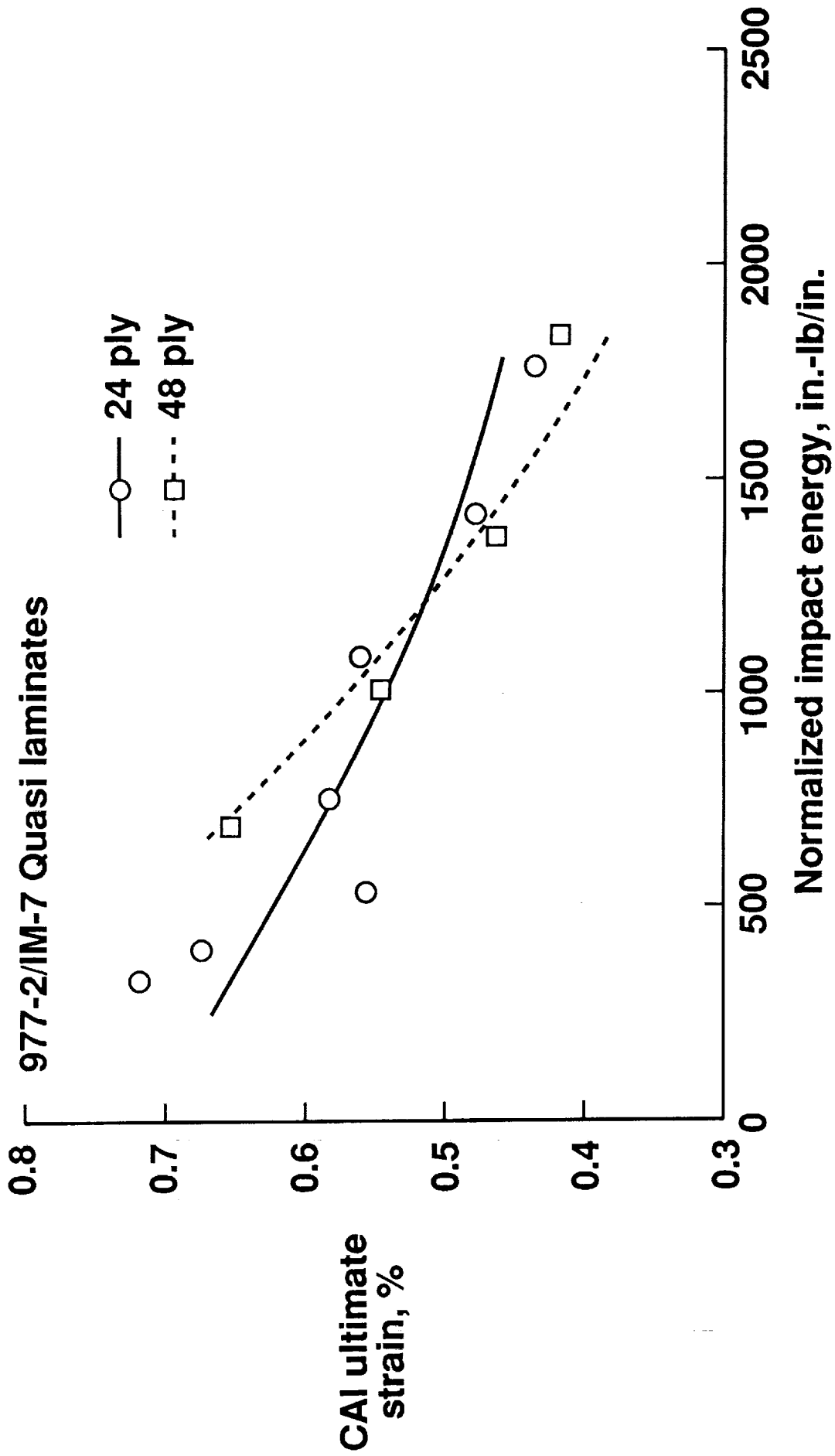
Figure 24. Influence of thickness on post-impact compression strains: 977-2.
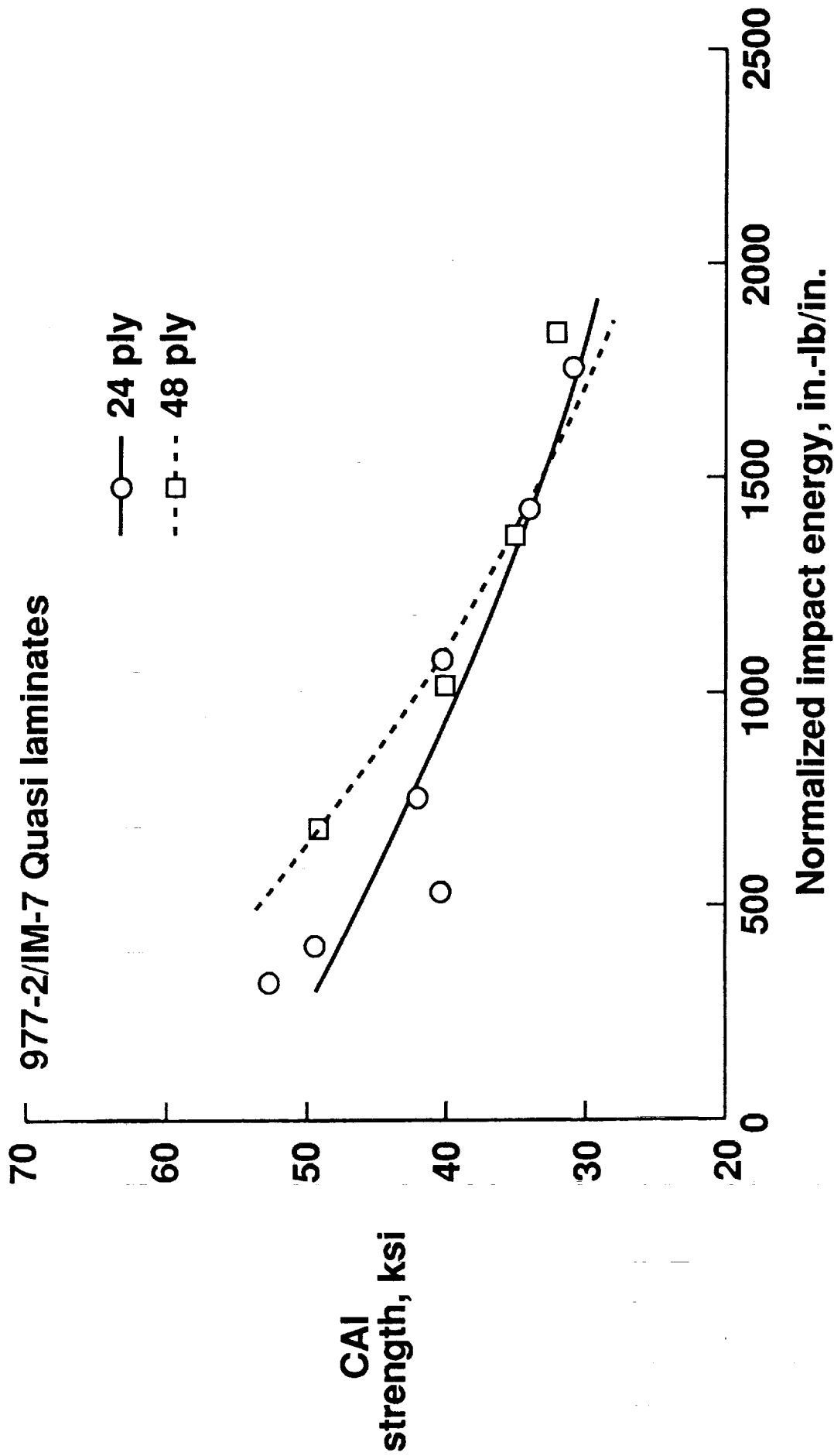
Figure 25. Influence of thickness on post-impact compression strengths: 977-2.

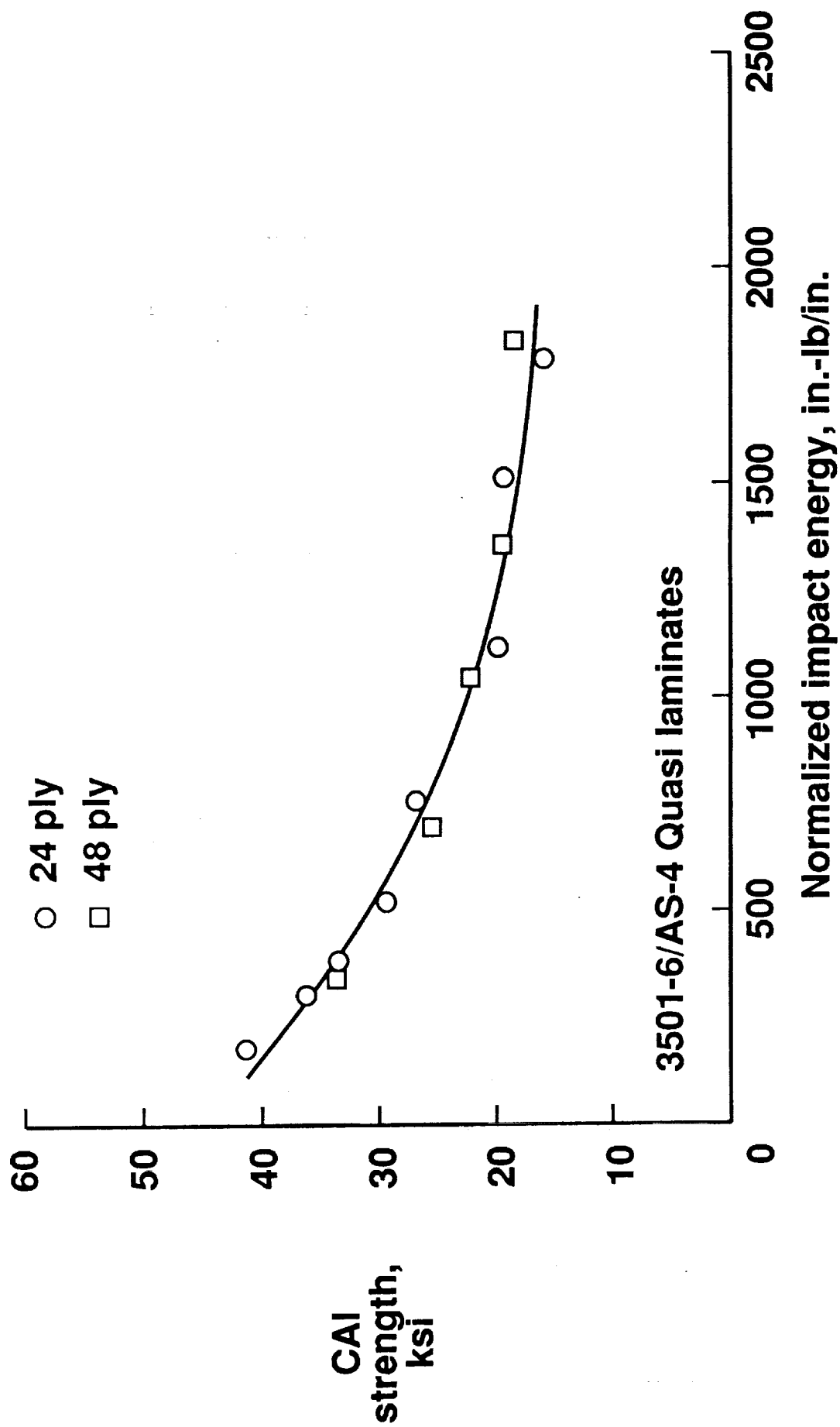Figure 26. Influence of thickness on post-impact compression strains: 3501-6.

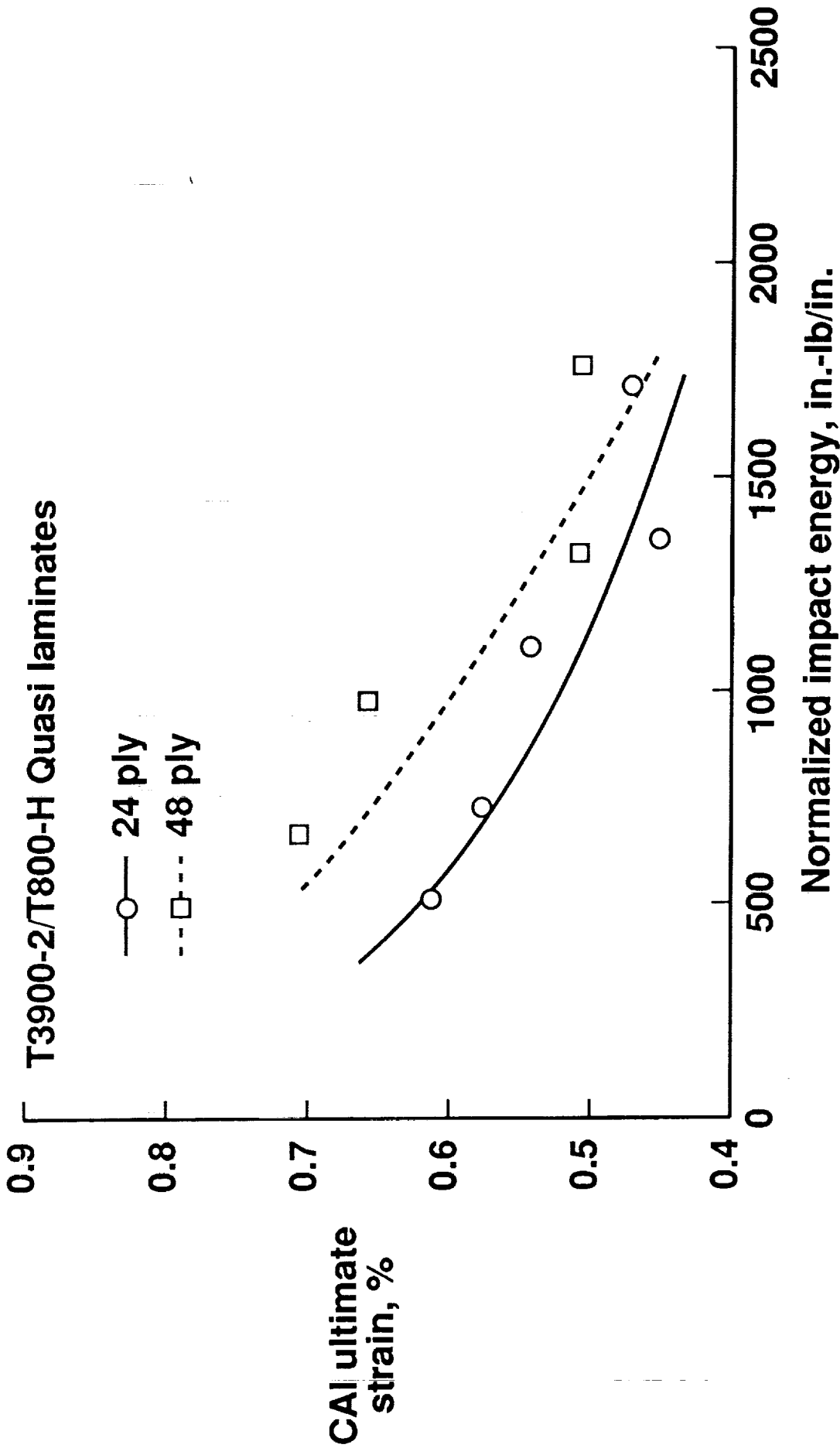Figure 27. Influence of thickness on post-impact compression strengths: 3501-6.

Figure 28. Influence of thickness on post-impact compression strains: T3900.
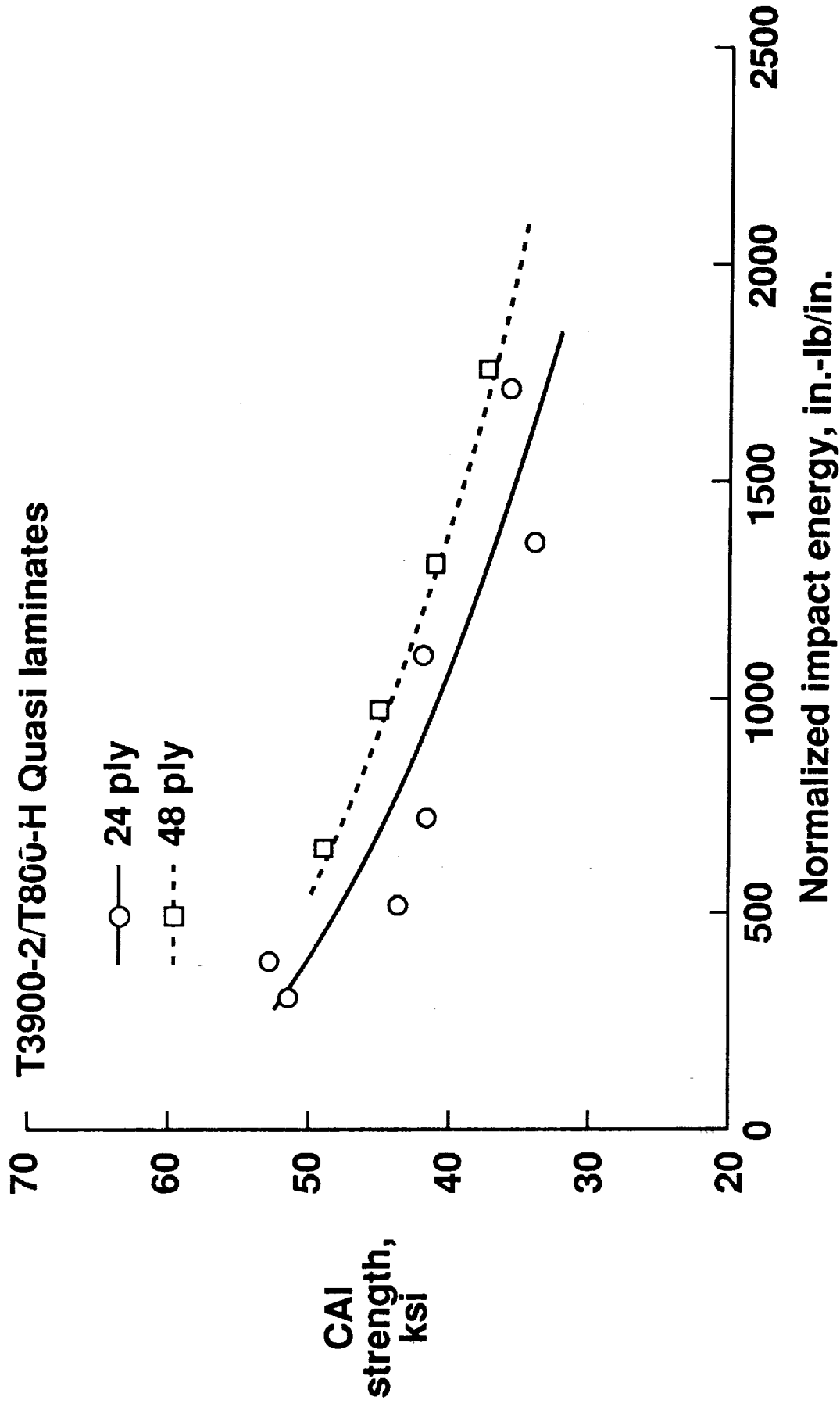
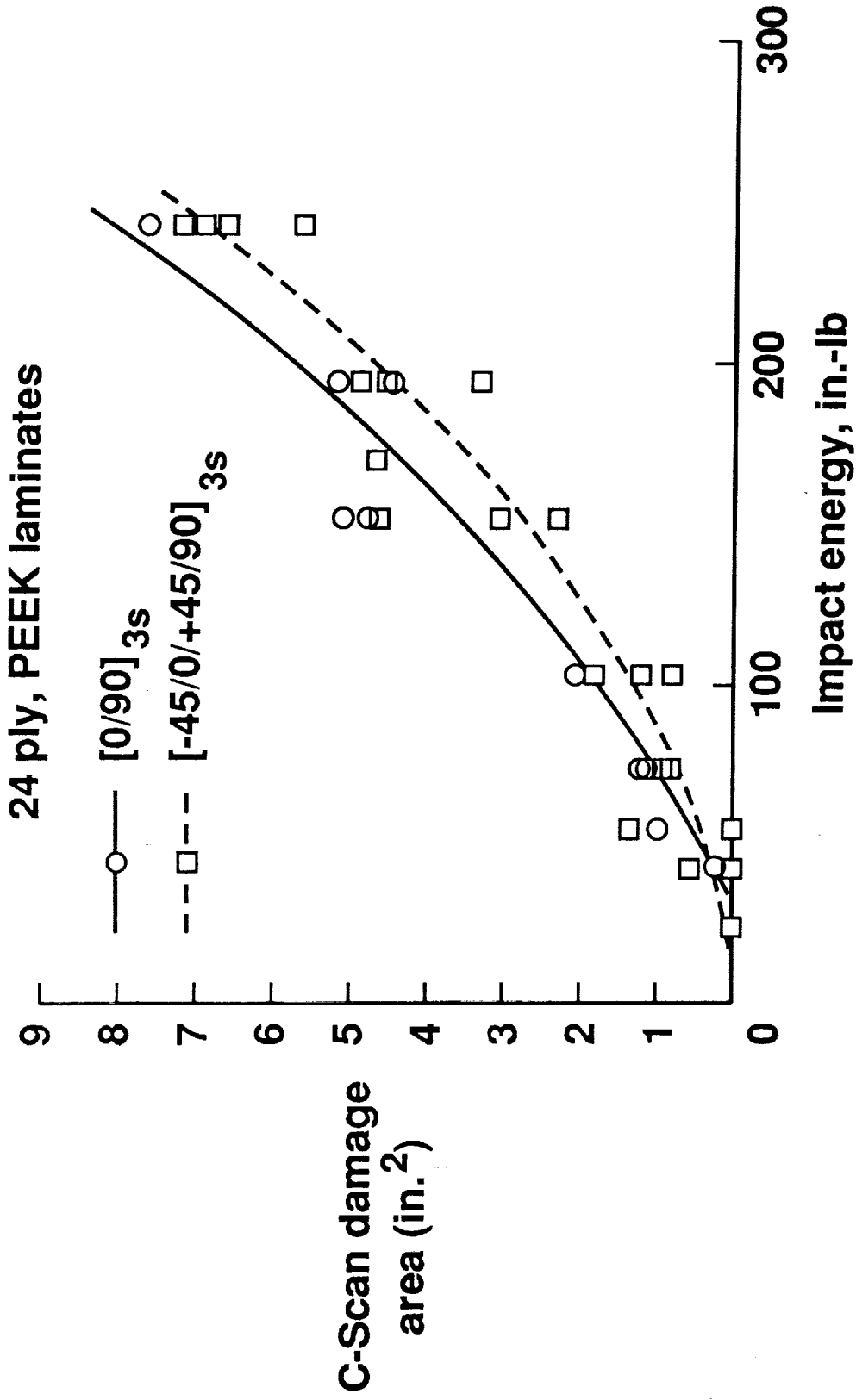Figure 29. Influence of thickness on post-impact compression strengths: T3900.

43

Figure 30. Comparison of C-scan damage areas of quasiisotropic and orthotropic PEEK laminates.

24 ply, PEEK laminates

Normalized CAI
ultimate strain

1.0

0.8

0.6

0.4

[0/90]$_{3s}$

[-45/0/+45/90]$_{3s}$
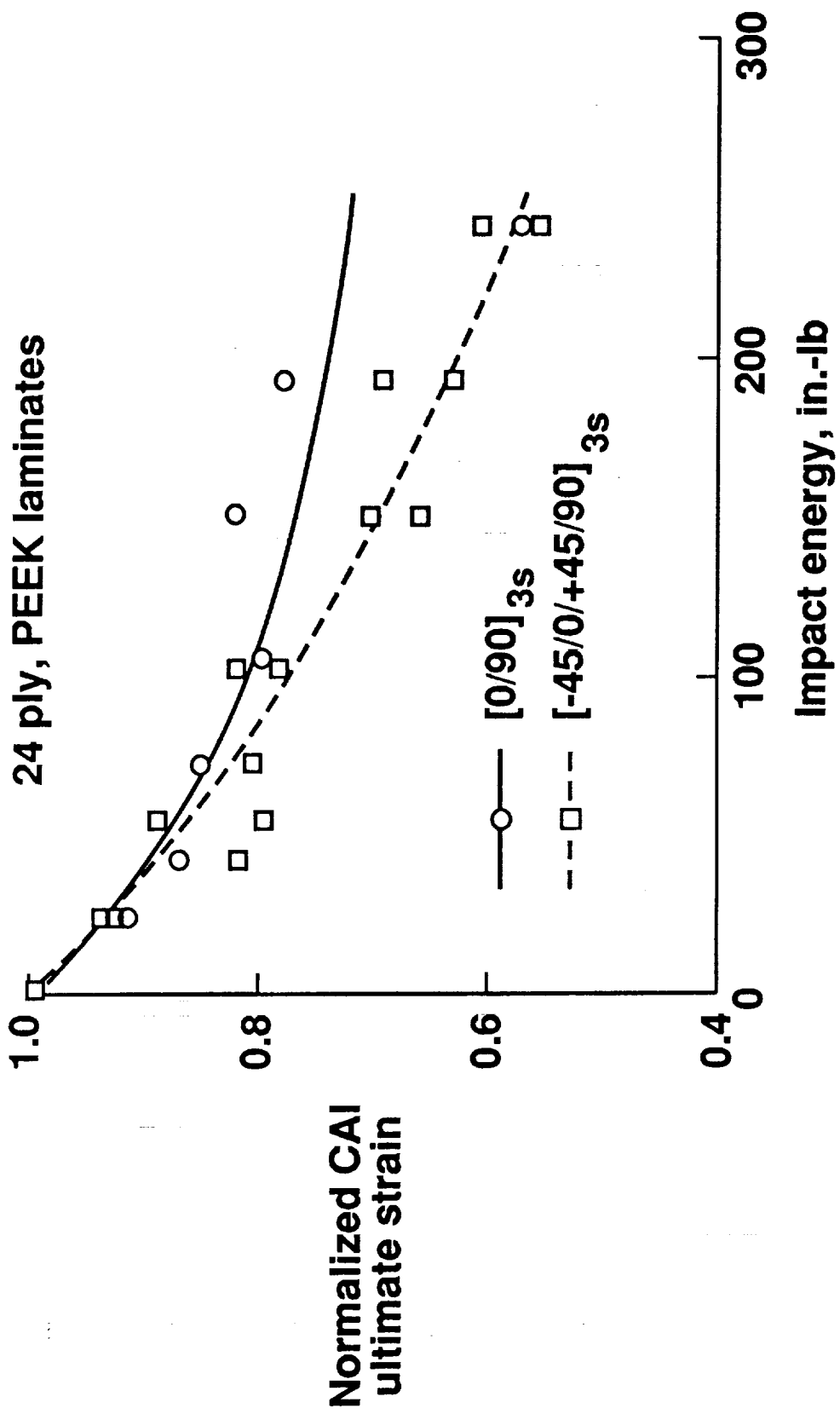
0   100   200   300

Impact energy, in.-lb

Figure 31. Comparison of post-impact compression strains of two different PEEK layups.
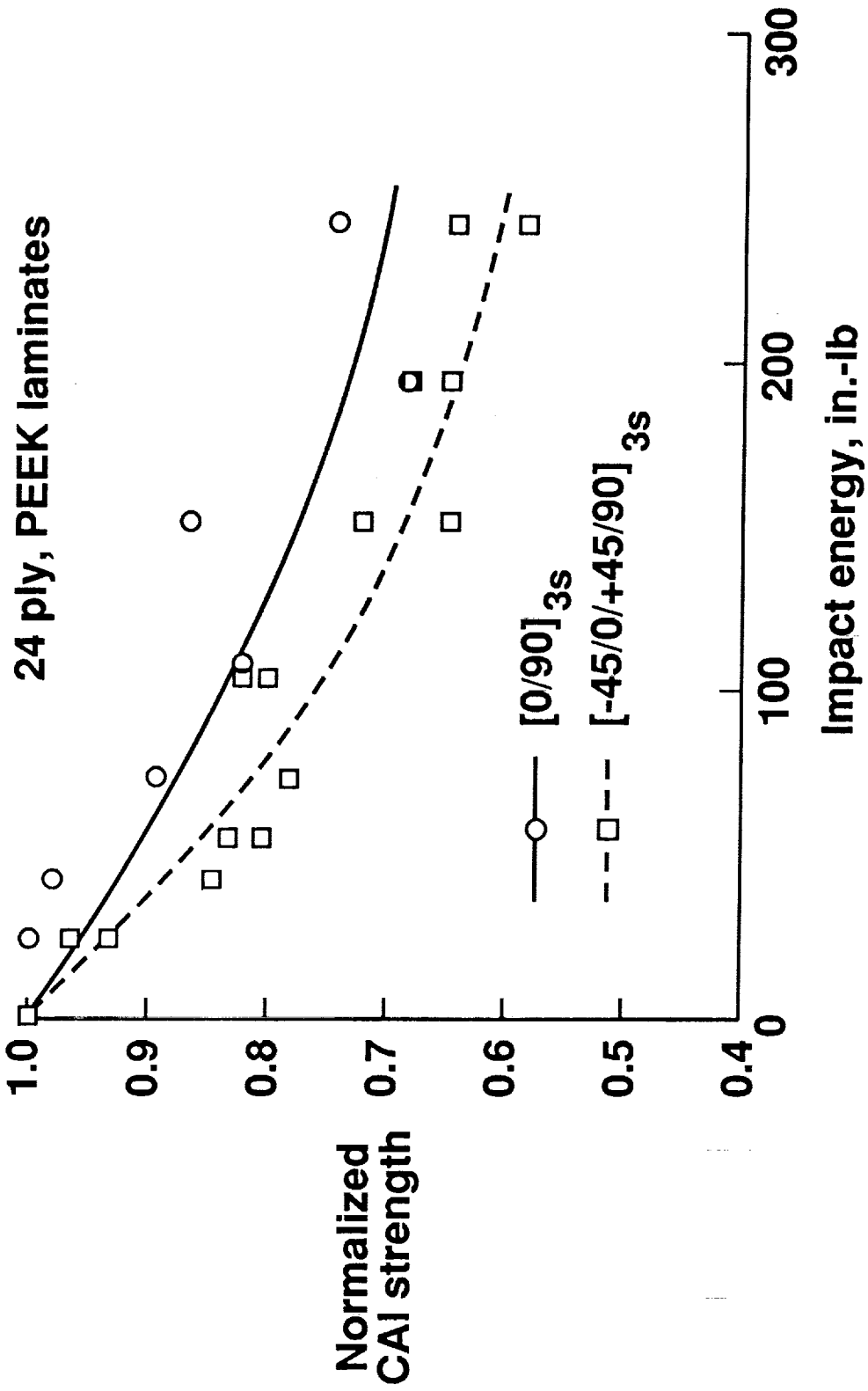
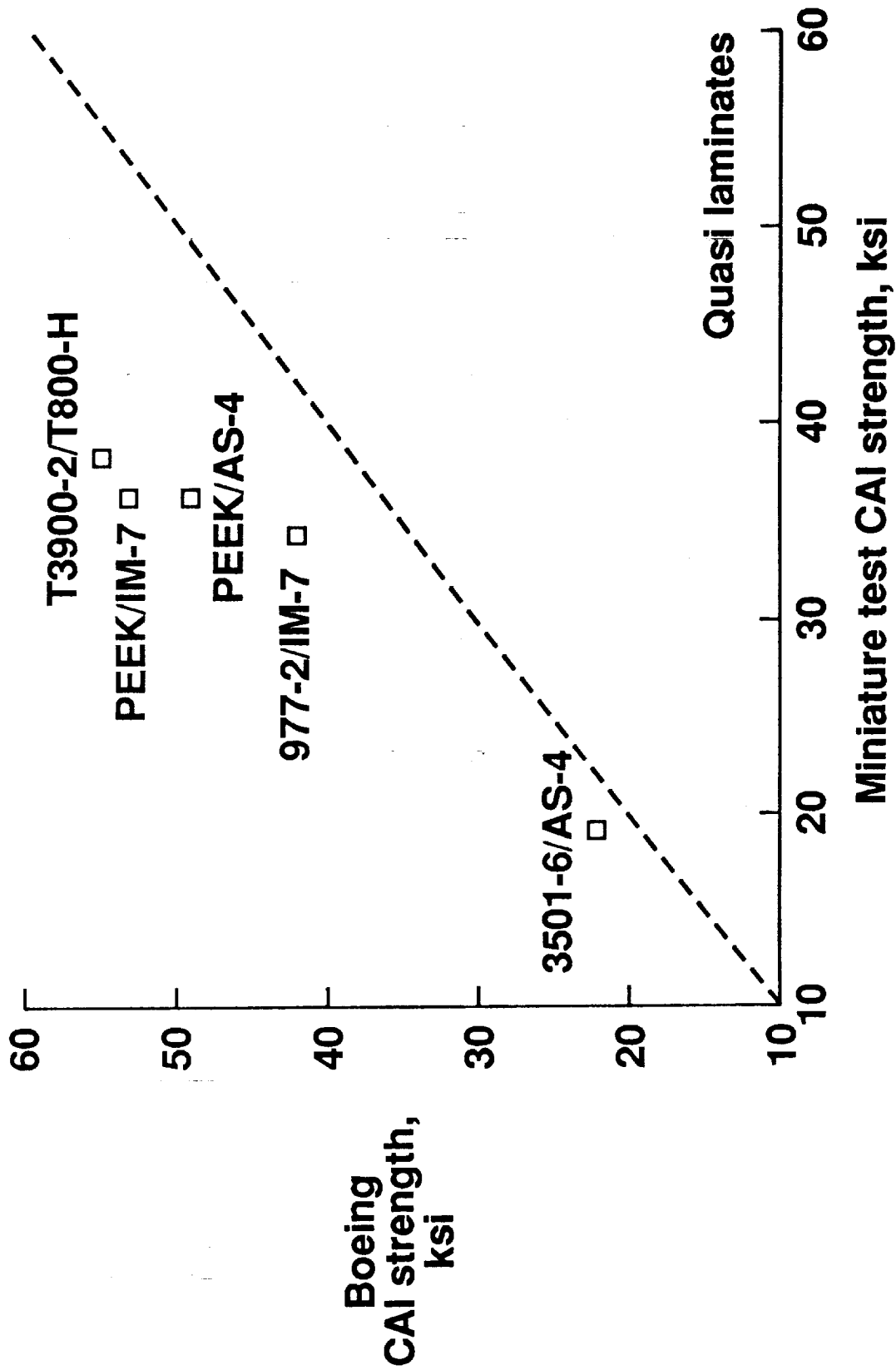Figure 32. Comparison of post-impact compression strengths for two different PEEK layups.

Figure 33. Comparison of present results with Boeing standard CAI test at 1500 in.-lb/in. impact energy.
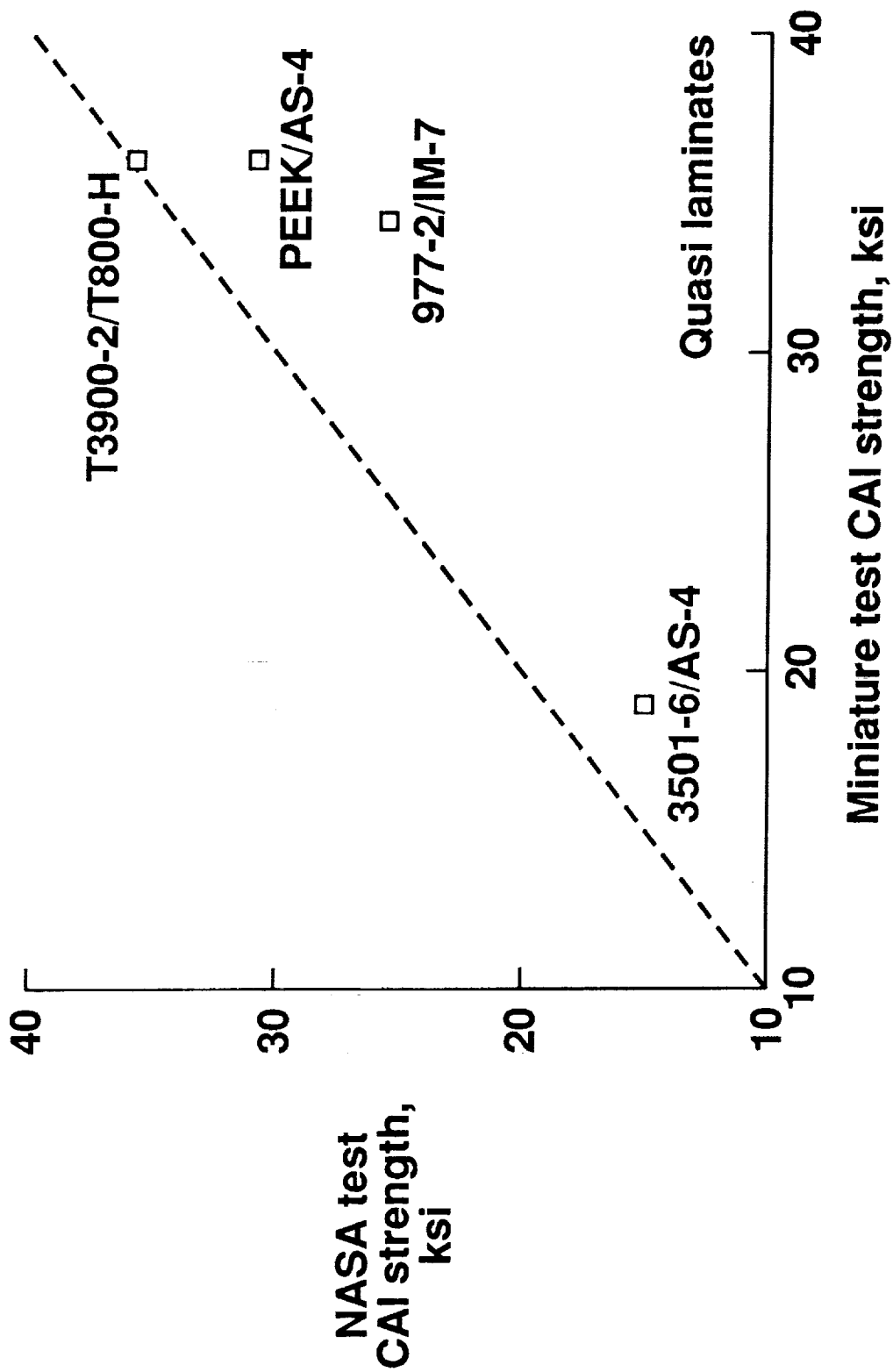
Figure 34. Comparison of present results with NASA CAI test at 1500 in.-lb/in. impact energy.

NASA National Aeronautics and Space Administration	Report Documentation Page	

1. Report No. NASA TM-102755 AVSCOM TM-90-B-018	2. Government Accession No.	3. Recipient's Catalog No.
4. Title and Subtitle Response of Composite Materials to Low Velocity Impact		5. Report Date January 1991
		6. Performing Organization Code
7. Author(s) K. Srinivasan, W. C. Jackson and J. A. Hinkley		8. Performing Organization Report No.
		10. Work Unit No. 505-63-50-01
9. Performing Organization Name and Address NASA Langley Research Center Hampton, VA 23665-5225 and Aerostructures Directorate, USAARTA-AVSCOM Langley Research Center, Hampton, VA 23665-5225		11. Contract or Grant No.
12. Sponsoring Agency Name and Address National Aeronautics and Space Administration Washington, DC 20546-0001 and U.S. Army Aviation Systems Command St. Louis, MO 63120-1798		13. Type of Report and Period Covered Technical Memorandum
		14. Sponsoring Agency Code

15. Supplementary Notes

K. Srinivasan: Old Dominion University, Norfolk, Virginia.
W. C. Jackson: Aerostructures Directorate, USAARTA-AVSCOM, Langley Research Center, Hampton, Virginia.
J. A. Hinkley: Langley Research Center, Hampton, Virginia.

16. Abstract

Orthotropic and quasiisotropic laminates clamped at the edges were impacted by an instrumented falling weight. Five matrix materials, comprising a baseline epoxy, two toughened thermosets, and amorphous and crystalline thermoplastics were studied. For each material, the projected damage area and residual compression strengths and strains were determined as a function of impact energy. Principal conclusions are 1) incipient damage associated with a prominent load drop during the impact test seems to be decisive for residual properties, 2) subtle rate effects are present with some materials and 3) results from the small scale tests parallel those in standard tests and may be adequate for screening purposes.

17. Key Words (Suggested by Author(s)) Damage tolerance Impact Compression-after-impact (CAI) Delamination Composites Damage resistance		18. Distribution Statement Unclassified - Unlimited Subject Category - 24	
19. Security Classif. (of this report) Unclassified	20. Security Classif. (of this page) Unclassified	21. No. of pages 49	22. Price A03

NASA FORM 1626 OCT 86